UNCLASSIFIED

AD NUMBER
AD886753
LIMITATION CHANGES

TO:

Approved for public release; distribution is unlimited.

FROM:

Distribution authorized to U.S. Gov't. agencies only; Test and Evaluation; AUG 1971. Other requests shall be referred to Armament Development and Test Center, Attn: DLDG, Eglin AFB, FL 32542.

AUTHORITY
AFATL ltr, 24 Jun 1974

THIS PAGE IS UNCLASSIFIED

SEPARATION CHARACTERISTICS OF THE MK-20 (ROCKEYE) LASER-GUIDED DISPENSER MUNITION FROM THE F-4C AIRCRAFT AT MACH NUMBERS FROM 0.65 TO 0.90

J. R. Myers

ARO, Inc.

August 1971

PROPULSION WIND TUNNEL FACILITY

ARNOLD ENGINEERING DEVELOPMENT CENTER

AIR FORCE SYSTEMS COMMAND

ARNOLD AIR FORCE STATION, TENNESSEE

NOTICES

SEPARATION CHARACTERISTICS OF THE MK-20 (ROCKEYE) LASER-GUIDED DISPENSER MUNITION FROM THE F-4C AIRCRAFT AT MACH NUMBERS FROM 0.66 TO 0.90

J. R. Myers
ARO, Inc.

FOREWORD

The work reported herein was sponsored by the Air Force Armament Laboratory (DLGC), Armament Development and Test Center (ADTC), Air Force Systems Command (AFSC), under Program Element 64724F, Project 1120, Task 09.

The test results presented were obtained by ARO, Inc. (a subsidiary of Sverdrup & Parcel and Associates, Inc.), contract operator of the Arnold Engineering Development Center (AEDC), AFSC, Arnold Air Force Station, Tennessee, under Contract F40600-72-C-0003. The test was conducted from May 10 to 13, 1971, under ARO Project No. PC0149. The manuscript was submitted for publication on June 9, 1971.

This technical report has been reviewed and is approved.

George F. Garey
Lt Colonel, USAF
AF Representative, PWT
Directorate of Test

Joseph R. Henry
Colonel, USAF
Director of Test

ABSTRACT

Wind-tunnel tests were conducted using 0.05-scale models to investigate the separation characteristics of the MK-20 Laser-Guided Rockeye Munition (GRM) from the F-4C aircraft. The separation trajectories were initiated from the right-wing inboard pylon utilizing the Triple Ejection Rack and from single carriage positions on the right-wing inboard and outboard pylons. Captive-trajectory store separation data were obtained at Mach numbers from 0.66 to 0.90 for parent-aircraft level flight and 45-deg dive angle at a simulated altitude of 5000 ft. Free-stream force and moment data were also obtained for the GRM with fins folded and deployed at Mach numbers from 0.66 to 0.90 at store angles of attack from -6 to 24 deg. For the time period of the trajectories obtained, the store separated from the parent aircraft without store-to-parent contact. Trajectory termination was usually a result of limitations imposed by the travel limits of the store support system or a balance load limit.

CONTENTS

APPENDIXES

I. ILLUSTRATIONS

Figure

NOMENCLATURE

BL   Aircraft buttock line from plane of symmetry, in., model scale

b   Store reference dimension, ft, full scale

C_m Store pitching-moment coefficient, referenced to the store cg, pitching moment/$q_\infty Sb$

C_{m_q} Store pitch-damping derivative, $dC_m/d(qb/2V_\infty)$

C_n Store yawing-moment coefficient, referenced to the store cg, yawing moment/$q_\infty Sb$

C_{n_r} Store yaw-damping derivative, $dC_n/d(rb/2V_\infty)$

FS   Aircraft fuselage station, in., model scale

F_Z MER/TER ejector force, lb

F_{Z_1} Pylon forward ejector force, lb

F_{Z_2} Pylon aft ejector force, lb

H   Pressure altitude, ft

I_{xz} Full-scale product of inertia, X_B - Z_B axis, slug-sq ft

I_{yy} Full-scale moment of inertia about the store Y_B axis, slug-sq ft

I_{zz} Full-scale moment of inertia about the store Z_B axis, slug-sq ft

M_∞ Free-stream Mach number

$\overline{m}$ Full-scale store mass, slugs

p_∞ Free-stream static pressure, psfa

q Store angular velocity about the Y_B axis, radians/sec

q_∞ Free-stream dynamic pressure, $0.7\, p_\infty M_\infty^2$, psf

r Store angular velocity about the Z_B axis. radians/sec

S Store reference area, sq ft, full scale

t Real trajectory time from initiation of trajectory, sec

V_∞ Free-stream velocity, ft/sec

WL   Aircraft waterline from reference horizontal plane, in., model scale

X Separation distance of the store cg parallel to the flight axis system X_F direction, ft, full scale measured from the prelaunch position

X_{cg} Full-scale cg location, ft, from nose of store

X_L Ejector piston location relative to the store cg, positive forward of store cg, ft, full scale

X_{L_1} Forward ejector piston location relative to the store cg, positive forward of store cg, ft, full scale

X_{L_2} Aft ejector piston location relative to the store cg, positive forward of store cg, ft, full scale

Y Separation distance of the store cg parallel to the flight-axis system Y_F direction, ft, full scale measured from the prelaunch position

Z Separation distance of the store cg parallel to the flight-axis system Z_F direction, ft, full scale measured from the prelaunch position

Z_E Ejector stroke length, ft, full scale

a Parent-aircraft or store model angle of attack relative to the free-stream velocity vector, deg

θ Angle between the store longitudinal axis and its projection in the X_F - Y_F plane, positive when store nose is raised as seen by pilot, deg

$\bar{\theta}$ Simulated parent-aircraft climb angle. Angle between the flight direction and the earth horizontal, deg, positive for increasing altitude

ψ Angle between the projection of the store longitudinal axis in the X_F - Y_F plane and the X_F axis, positive when the store nose is to the right as seen by the pilot, deg

FLIGHT-AXIS SYSTEM COORDINATES

Directions

X_F Parallel to the free-stream wind vector, positive direction is forward as seen by the pilot

Y_F Perpendicular to the X_F and Z_F directions, positive direction is to the right as seen by the pilot

Z_F In the aircraft plane of symmetry, perpendicular to the free-stream wind vector, positive direction is downward

       The flight-axis system origin is coincident with the aircraft cg and remains fixed with respect to the parent aircraft during store separation. The X_F, Y_F, and Z_F coordinate axes do not rotate with respect to the initial flight direction and attitude.

STORE BODY-AXIS SYSTEM COORDINATES

Directions

X_B Parallel to the store longitudinal axis, positive direction is upstream in the prelaunch position

Y_B Perpendicular to the store longitudinal axis, and parallel to the flight-axis system X_F - Y_F plane when the store is at zero roll angle, positive direction is to the right looking upstream when the store is at zero yaw and roll angles

Z_B Perpendicular to both the X_B and Y_B axes, positive direction is downward as seen by the pilot when the store is at zero pitch and roll angles.

       The store body-axis system origin is coincident with the store cg and moves with the store during separation from the parent airplane. The X_B, Y_B, and Z_B coordinate axes rotate with the store in pitch, yaw, and roll so that mass moments of inertia about the three axes are not time-varying quantities.

SECTION I
INTRODUCTION

This investigation was conducted in the Aerodynamic Wind Tunnel (4T) of the Propulsion Wind Tunnel Facility to obtain captive-trajectory store-separation data for the Guided Rockeye Munition (GRM) when released from various F-4C multiple- and single-carriage configurations. Separation trajectories for the multiple-carriage configurations utilized the folded-fin model and were initiated from the launch position with a simulated ejector force. If the trajectory was of sufficient length to reach the position where the fins could be deployed, the open-fin configuration was used to obtain additional data starting from the chosen store location along the original trajectory. The criterion for fin deployment was a clearance of approximately 1 ft, full scale, between the rack and the aft end of the store. Some trajectories were terminated a very short time after fin deployment because of store support system travel limits resulting from high pitch or yaw angles. These short open-fin-configuration trajectory continuations are not presented. Separation trajectories from the single-carriage inboard and outboard pylon stations were initiated from their launch position with simulated forward and aft ejector forces. The open-fin store configuration was used throughout the single-carriage phase of testing.

The test was conducted using 0.05-scale models of the F-4C parent aircraft mounted to the main tunnel support system and of the GRM store mounted on a strain-gage balance-and-sting combination attached to the Captive Trajectory Support (CTS) system. Flight conditions simulated were Mach numbers from 0.66 to 0.90, an altitude of 5000 ft, and parent-aircraft climb angles of 0 and -45 deg.

Free-stream static stability data for the fins-folded and fins-deployed models were obtained at Mach numbers from 0.66 to 0.90 at store angles of attack from -6 to 24 deg.

SECTION II
APPARATUS

2.1 TEST FACILITY

The Aerodynamic Wind Tunnel (4T) is a closed-loop, continuous flow, variable density tunnel in which the Mach number can be varied from 0.2 to 1.3. At all Mach numbers, the stagnation pressure can be varied from 200 to 3400 psfa. The test section is 4 ft square and 12.5 ft long with perforated, variable porosity (0.5- to 10-percent open) walls. It is completely enclosed in a plenum chamber from which the air can be evacuated, allowing part of the tunnel airflow to be removed through the perforated walls of the test section.

For store-separation testing, two separate and independent support systems are used to support the models. The parent-aircraft model is inverted in the test section and supported by an offset sting attached to the main pitch sector. The store model is supported by the CTS which extends down from the tunnel top wall and provides store movement (six degrees of freedom) independent of the parent-aircraft model. An isometric drawing of a typical store separation installation is shown in Fig. 1, Appendix I.

Also shown in Fig. 1 is a block diagram of the computer control loop used during captive trajectory testing. The analog system and the digital computer work as an integrated unit and, utilizing required input information, control the store movement during a trajectory. Store positioning is accomplished by use of six individual d-c electric motors. Maximum translational travel of the CTS is ±15 in. from the tunnel centerline in the lateral and vertical directions and 36 in. in the axial direction. Maximum angular displacements are ±45 deg in pitch and yaw and ±360 deg in roll. A more complete description of the test facility can be found in the Test Facilities Handbook.[1] A schematic showing the test section details and the location of the models in the tunnel is shown in Fig. 2.

2.2 TEST ARTICLES

The test articles were 0.05-scale models of the F-4C parent aircraft and the MK-20 Laser-Guided Dispenser GRM store. A sketch showing the basic dimensions of the F-4C parent model is shown in Fig. 3. For this test, the right wing and fuselage centerline of the F-4C model were equipped for store separation. The tail of the F-4C model was removed to provide clearance for the CTS. Details and dimensions of the pylons are shown in Fig. 4. The surfaces of the pylons are inclined nose-down with respect to the aircraft waterline as indicated in Fig. 4.

The Triple Ejection Rack (TER) and Multiple Ejection Rack (MER) were mounted on the inboard and centerline pylons, respectively, and matched to the 30-in. suspension lugs of the pylons. The MER was mounted in the forward-shifted position on the fuselage centerline pylon. Details and dimensions of the TER and MER are shown in Figs. 5 and 6, respectively.

Details and dimensions of the GRM store model are shown in Fig. 7. Dimensional sketches of the 370- and 600-gal dummy fuel tanks used to simulate the desired aircraft configurations are shown in Figs. 8 and 9, respectively. Figure 10 is a tunnel installation photograph showing the parent aircraft with stores and the CTS. Aircraft/weapons loading nomenclature is given in Fig. 11, and the loading configurations for which trajectory data were obtained are shown in Fig. 12.

2.3 INSTRUMENTATION

A five-component. internal strain-gage balance was used to obtain the force and moment data on the GRM model. Translational and angular positions of the store model were obtained from the CTS analog outputs. An angular position indicator on the main pitch sector was used to determine the parent-model angle of attack. Touch wires were located in the racks and pylons in order to provide a position indication when the store model was in the launch position. The CTS was electrically connected to automatically stop and give a visual indication if the store model or sting contacted the parent-aircraft surface.

---

[1]Test Facilities Handbook (Ninth Edition). "Propulsion Wind Tunnel Facility, Vol. 5." Arnold Engineering Development Center, July 1971.

SECTION III
TEST DESCRIPTION

3.1 TEST CONDITIONS

Separation trajectory data were obtained at Mach numbers from 0.66 to 0.90. Tunnel dynamic pressure was 500 psf at all Mach numbers, and tunnel stagnation temperature was maintained near 110°F.

Tunnel conditions were held constant at the desired Mach number and stagnation pressure while data for each trajectory were obtained. The trajectories were terminated when the store or sting contacted the parent-aircraft model or when a CTS limit was reached.

3.2 TRAJECTORY DATA ACQUISITION

To obtain a trajectory, test conditions were established in the tunnel and the parent model was positioned at the desired angle of attack. The store model was then oriented to a position corresponding to the store carriage location. After the store was set at the desired initial position, operational control of the CTS was switched to the digital computer which controlled the store movement during the trajectory through commands to the CTS analog system (see block diagram, Fig. 1). Data from the wind tunnel, consisting of measured model forces and moments, wind-tunnel operating conditions, and CTS rig positions were input to the digital computer for use in the full-scale trajectory calculations.

The digital computer was programmed to solve the six-degree-of-freedom equations to calculate the angular and linear displacements of the store relative to the parent-aircraft pylon. In general, the program involves using the last two successive measured values of each static aerodynamic coefficient to predict the magnitude of the coefficients over the next time interval of the trajectory. These predicted values are used to calculate the new position and attitude of the store at the end of the time interval. The CTS is then commanded to move the store model to this new position and the aerodynamic loads are measured. If these new measurements agree with the predicted values, the process is continued over another time.interval of the same magnitude. If the measured and predicted values do not agree within the desired precision, the calculation is redone over a time interval one-half the previous value. This process is repeated until a complete trajectory has been obtained.

In applying the wind-tunnel data to the calculations of the full-scale store trajectories, the measured forces and moments are reduced to coefficient form and then applied with proper full-scale store dimensions and flight dynamic pressure. Dynamic pressure was calculated using a flight velocity equal to the free-stream velocity component plus the components of store velocity relative to the aircraft, and a density corresponding to the simulated altitude.

3

The initial portion of each launch trajectory incorporated simulated ejector forces in addition to the measured aerodynamic forces acting on the store. The ejector force functions for the GRM on the TER and pylons are presented in Fig. 13. The ejector force was considered to act perpendicular to the rack or pylon mounting surface. The locations of the applied ejector forces and other full-scale store parameters used in the trajectory calculations are listed in Table I, Appendix II.

3.3 CORRECTIONS

Balance, sting, and support deflections caused by the aerodynamic loads on the store models were accounted for in the data reduction program to calculate the true store-model angles. Corrections were also made for model weight tares to calculate the net aerodynamic forces on the store model.

3.4 PRECISION OF DATA

The trajectory data are subject to error from several sources including tunnel conditions, balance measurements, extrapolation tolerances allowed in the predicted coefficients, computer inputs, and CTS positioning control. Maximum error in the CTS position control was ±0.05 in. for the translational settings and ±0.15 deg for angular displacement settings in pitch and yaw. Extrapolation tolerances were ±0.10 for each of the aerodynamic coefficients. The maximum uncertainties in the full-scale position data caused by the balance precision limitations are given in Table II.

The estimated uncertainty in setting Mach number was ±0.003, and the uncertainty in parent-model angle of attack was estimated to be ±0.1 deg.

<div align="center">

SECTION IV
RESULTS AND DISCUSSION

</div>

Data obtained during this test consisted of ejector-separated trajectories of the Guided Rockeye Muntion (GRM) from inboard multiple-carriage and inboard/outboard single-carriage stations on the right wing of the F-4C aircraft. Data showing the linear displacements of the stores relative to the carriage position, and the angular displacements relative to the flight-axis system, are presented as functions of full-scale trajectory time in Figs. 14 through 23. Positive X, Y, and Z displacements (as seen by the pilot) are forward, to the right (outboard), and down, respectively. Positive changes in θ and ψ (as seen by the pilot) are nose up and nose right (outboard), respectively. Multiple-carriage separation trajectories for a parent-aircraft dive angle of 45 deg included trajectories that referenced the aerodynamic moments to a point forward of the GRM center-of-gravity. The forward shift of 1 cal (1.100-ft full scale) in moment center (denoted as F on the data plots) from the normal position (denoted as N on the data plots) was a stabilizing maneuver which simulated an increased fin area of the store. Termination of the trajectories was usually a result of limitations imposed by the CTS system, such as sting-to-parent-aircraft contact, a CTS travel limit, or a balance load limit. Table I lists the full-scale store parameters used in the trajectory calculations and Fig. 12 describes the F-4C load configurations.

The ejector force functions used with the TER and pylons were supplied by the sponsor (ADTC) and are shown in Fig. 13. The TER ejector force was terminated when the store had moved away a distance equal to the ejector piston stroke length (see Table I). For the pylon ejector forces, the force functions were terminated at a trajectory time of 0.043 sec, at which time the forces had diminished essentially to zero.

Figures 14 through 21 present data for launches from TER stations on the wing inboard pylon, and are presented for the various Mach numbers at which the test was conducted at dive angles of 0 and 45 deg. and 45 deg with a forward-shifted moment reference. Configurations 1 and 3 represent mirror images of launches from the left-wing inboard pylon and configurations 2 and 4 represent right-wing launches. Figures 14 through 17 present data for configurations with folded fins. All separation trajectories exhibited an initial nose-down pitch motion which was more rapid at the higher Mach numbers. For Configurations 1 and 2, where the store was in the presence of an opposite dummy store, the yaw motion was away from the dummy store. For Configurations 3 and 4, with no opposite dummy store, the store exhibited a lower rate of yaw with the direction depending on Mach number. Figures 18 through 21 show the influence of deploying the fins when the store aft end was approximately 1 ft from the rack. Testing with the fins open, forward-shifted moment center, was limited to Configurations 1 and 2. Other trajectories for the regular test conditions are not shown because the CTS travel limits had been reached after a very short time interval. The fins were only partially effective in stabilizing the store for the trajectories with the normal-moment center.

Single-carriage, open-fin separation trajectory data from the outboard and inboard pylons are presented in Figs. 22 and 23, respectively. Store separations from the outboard pylon exhibited unstable motion in both pitch and yaw.

Free-stream static stability data are presented in Fig. 24 for the GRM folded-fin and open-fin models. The stabilizing effectiveness of the open fins was irregular, and was reduced at angles of attack greater than 8 deg. The model became unstable at angles of attack near 20 deg at the lower Mach numbers.

APPENDIXES
I. ILLUSTRATIONS
II. TABLES
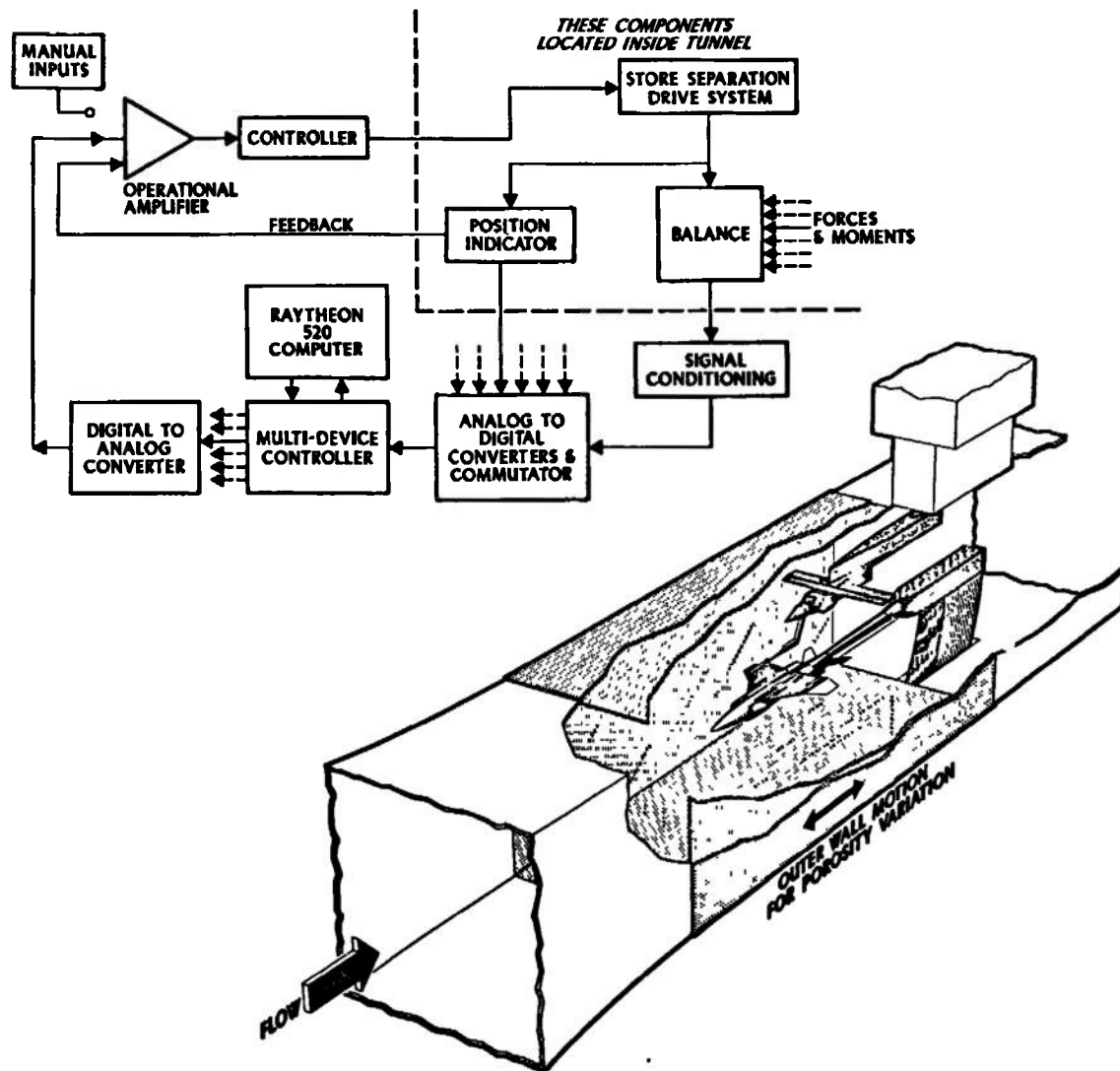
Fig. 1 Isometric Drawing of a Typical Store Separation Installation and a
Block Diagram of the Computer Control Loop

60°

0.500 DIAM

AIRSTREAM SURFACE

0.375

0.375
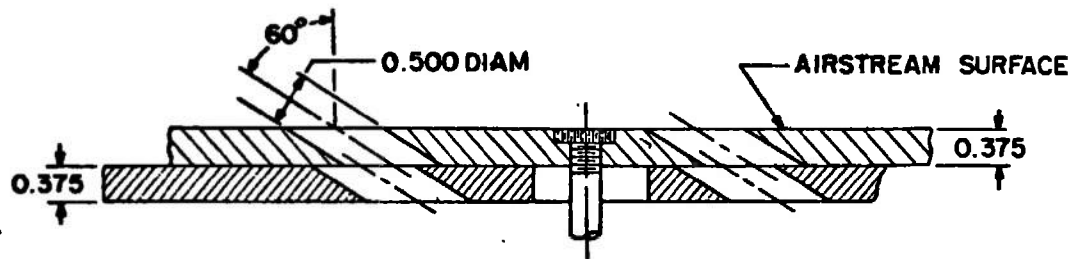
TYPICAL PERFORATED WALL CROSS SECTION

TUNNEL STATIONS AND DIMENSIONS
IN INCHES

SOLID AREAS

PERFORATED WALLS (10 % MAXIMUM OPEN AREA)

CTS STING SUPPORT

F-4
MODEL

STORE

₵

FLOW
EXPANSION
REGION

STA.
0.0

STA.
36.0

STA.
90.1

STA.
150.0
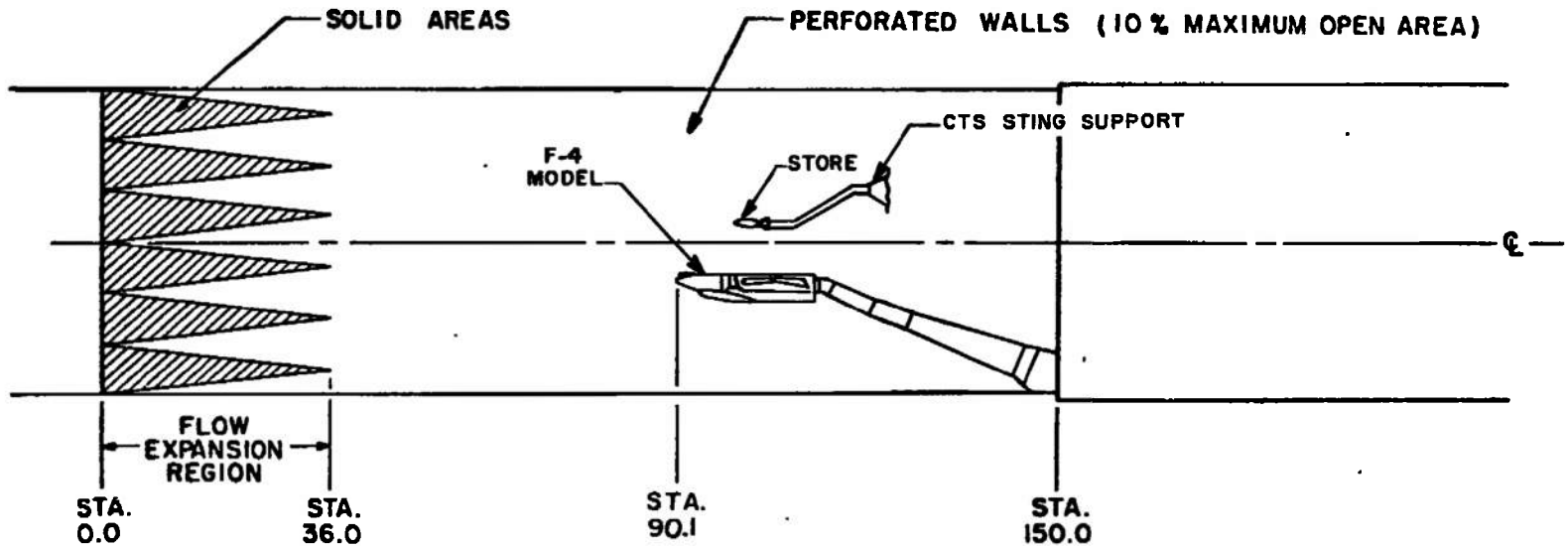
Fig. 2 Schematic of the Tunnel Test Section Showing Model Location

WL 0000

BL 11.560

BL 6 625

BL 4.075

BL-4 075
INBOARD PYLON

BL-6 625
OUTBOARD PYLON

BL-11 560

FS-1 355
FS 0 000

FS 33 166

STATIONS IN INCHES
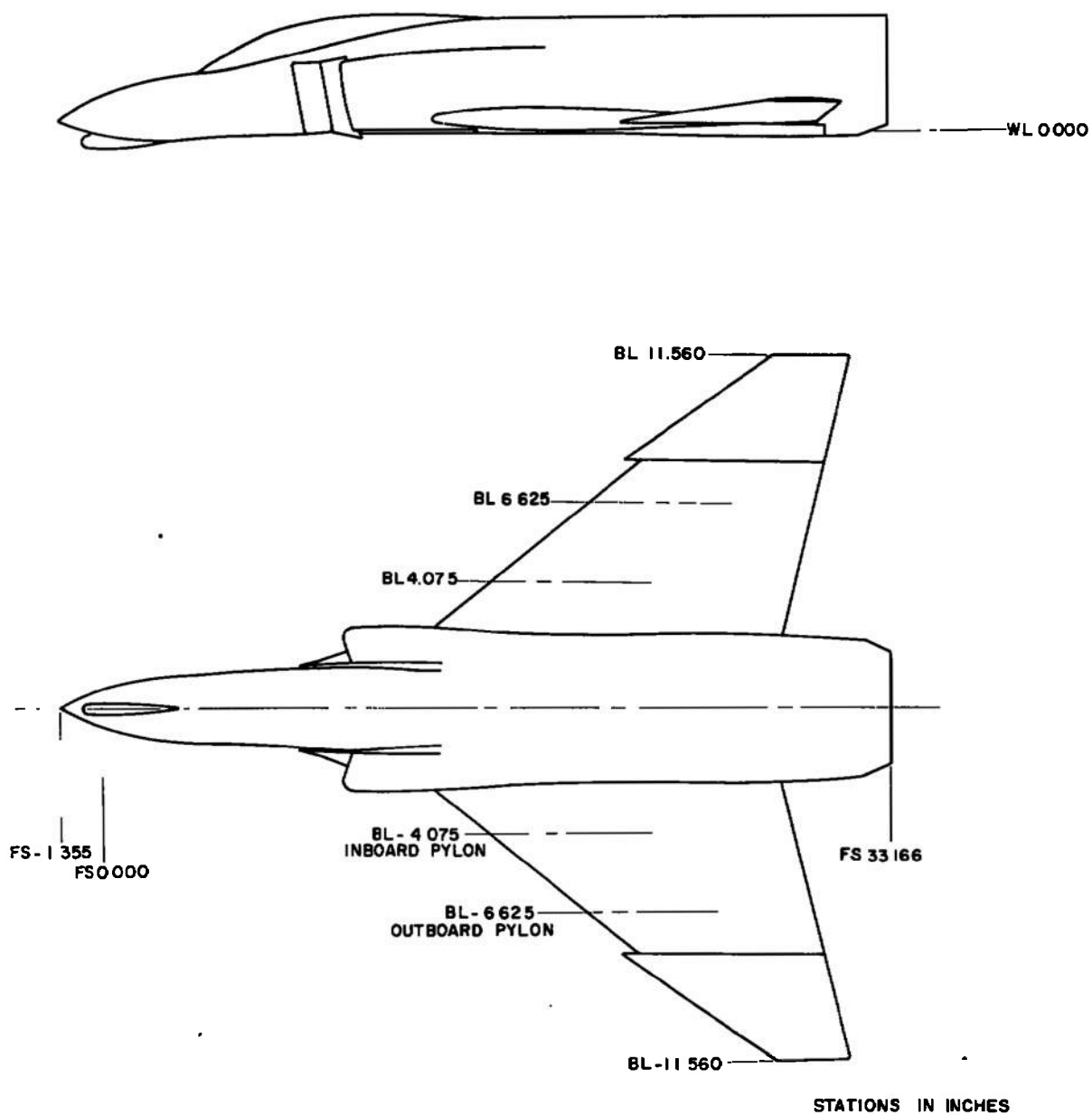
Fig. 3 Sketch of the F-4C Parent-Aircraft Model

11
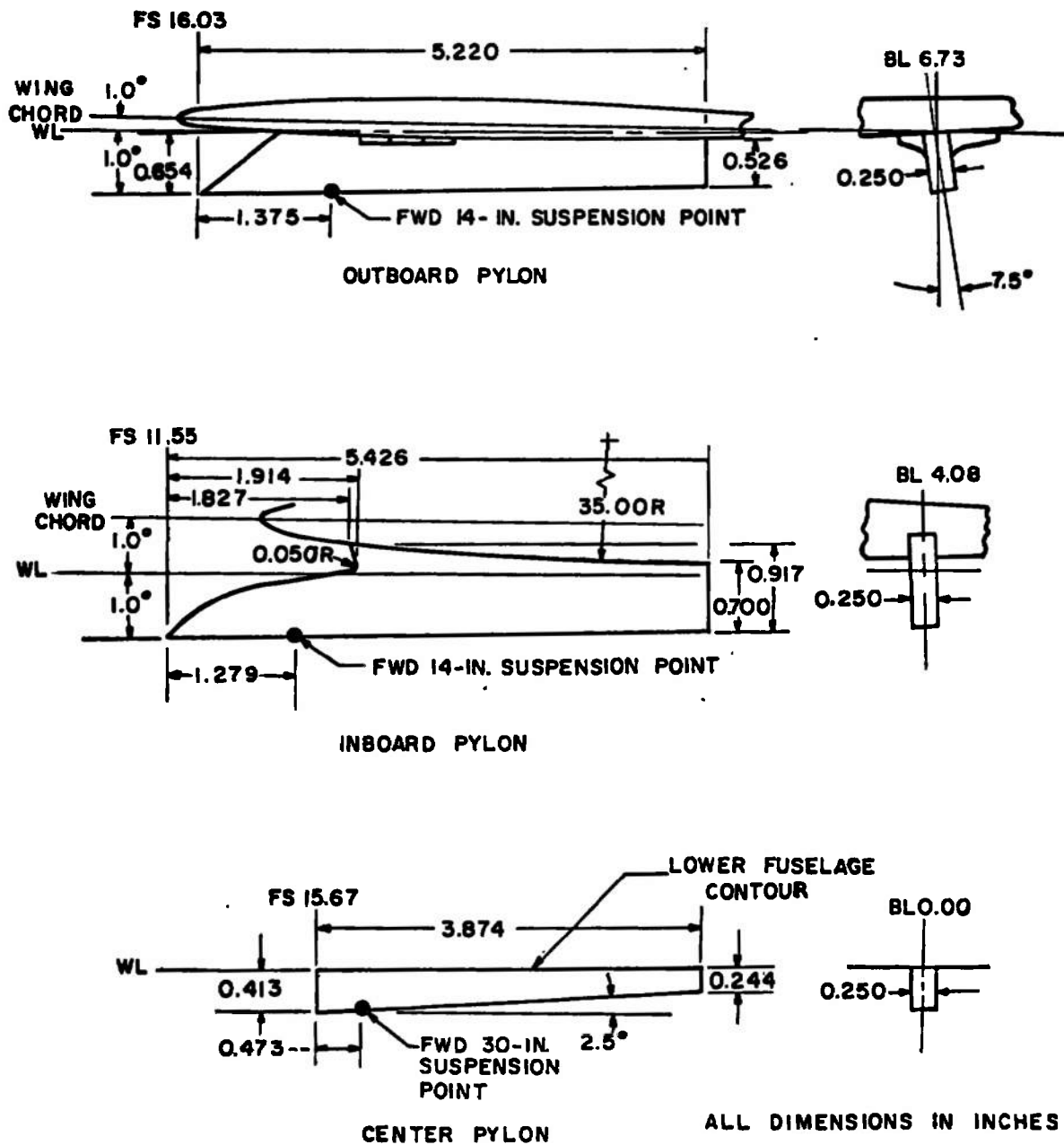
Fig. 4 Details and Dimensions of the F-4C Pylon Models
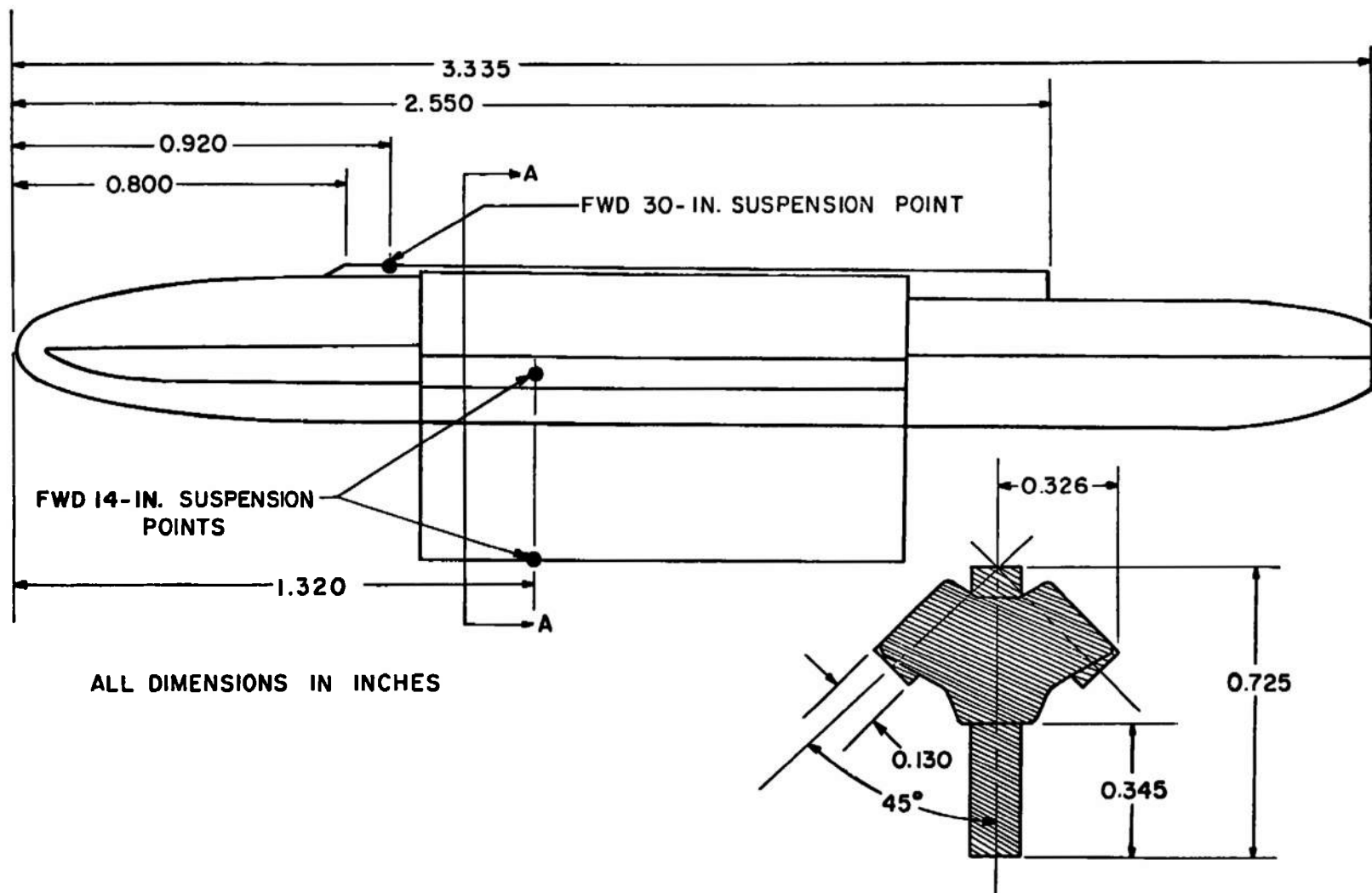
Fig. 5 Details and Dimensions of the TER Model

3.335

2.550

0.920

0.800

A

FWD 30-IN. SUSPENSION POINT

FWD 14-IN. SUSPENSION POINTS

1.320

A

ALL DIMENSIONS IN INCHES

0.326

0.725

0.130

0.345

45°
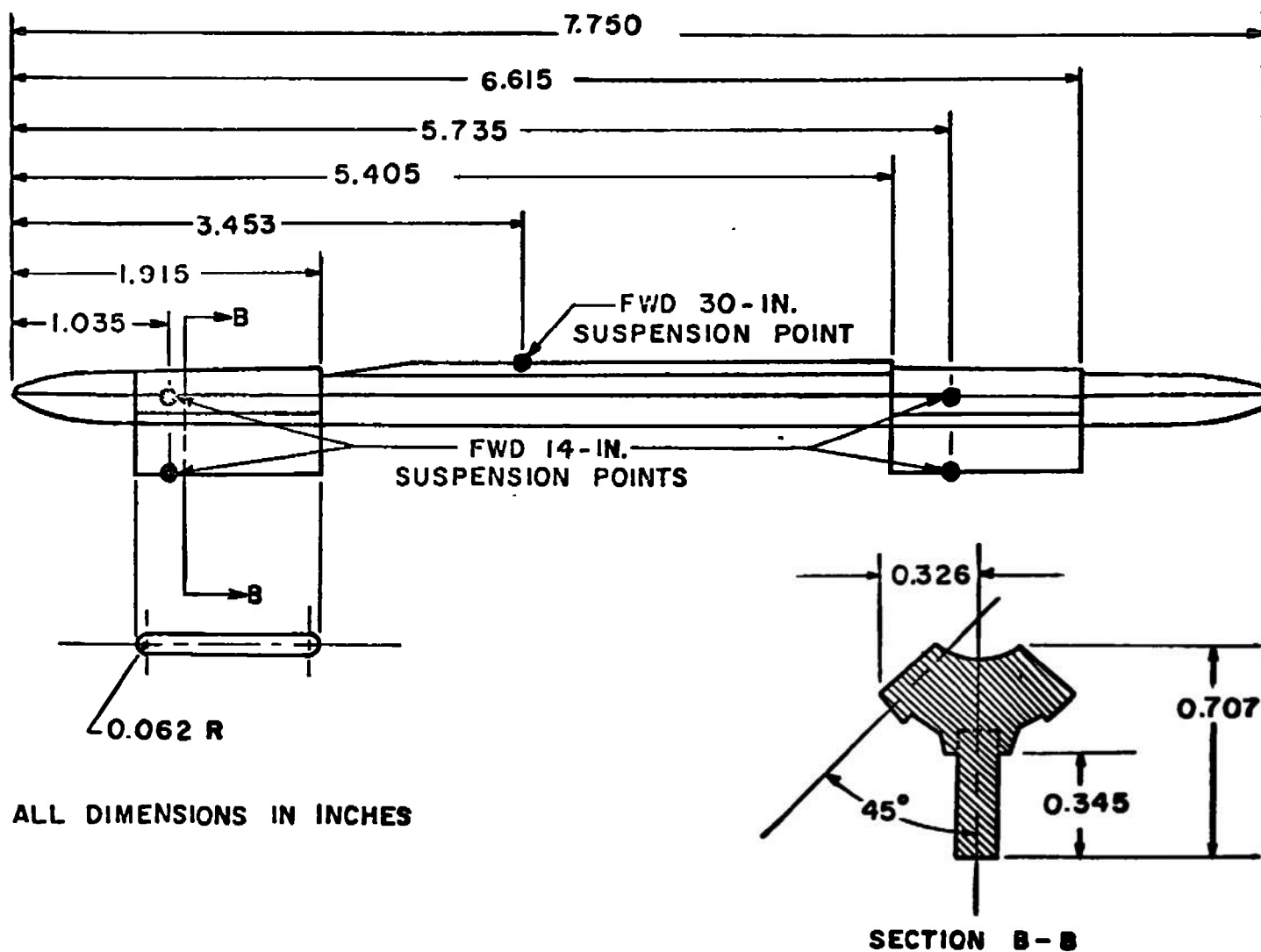
Fig. 6 Details and Dimensions of the MER Model
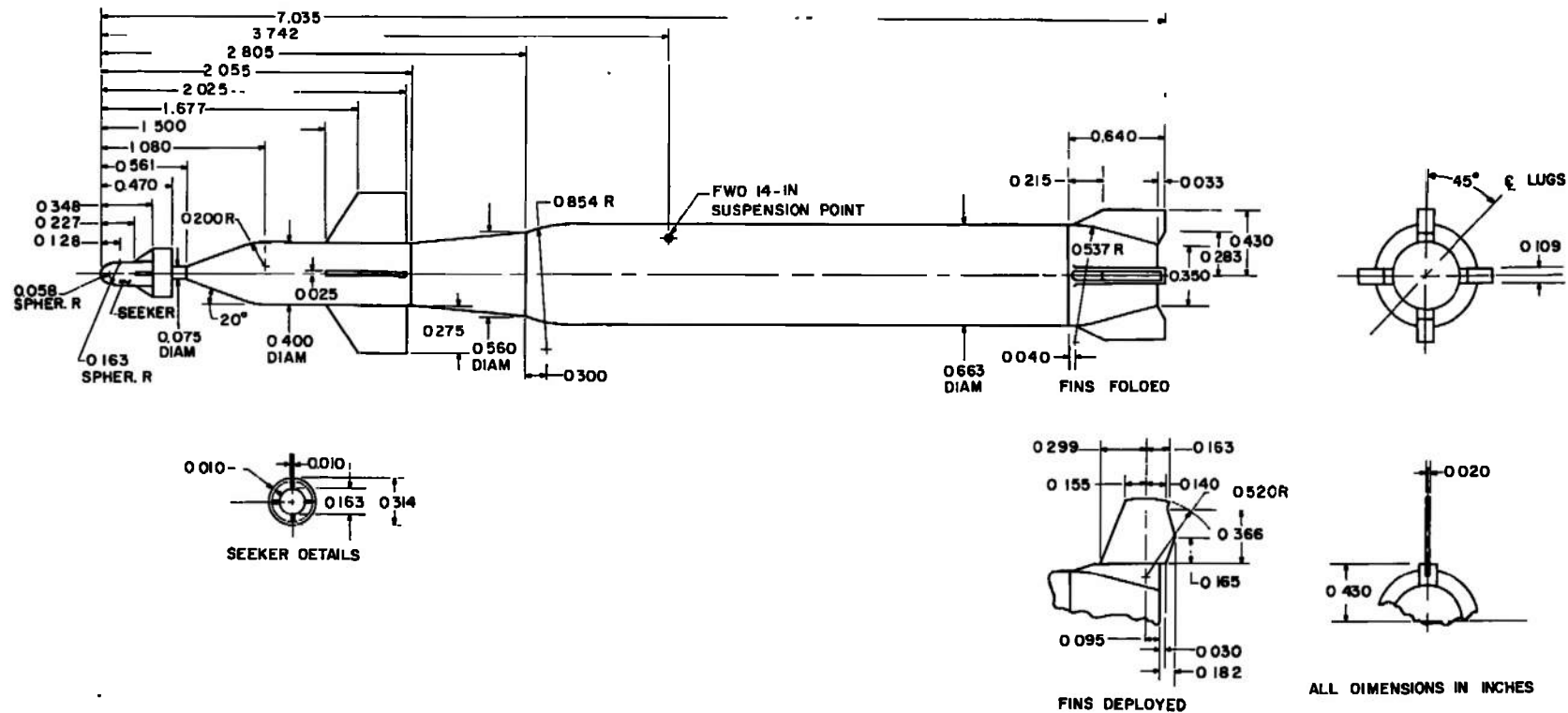
Fig. 7 Details and Dimensions of the GRM Model

FS 10.652

FS 16.050

0.500

WL

1.5°

0.480

12.000

STA 0.0

BL 6.730

7.5°

INBOARD

1.300

ALL DIMENSIONS AND MODEL STATIONS IN INCHES
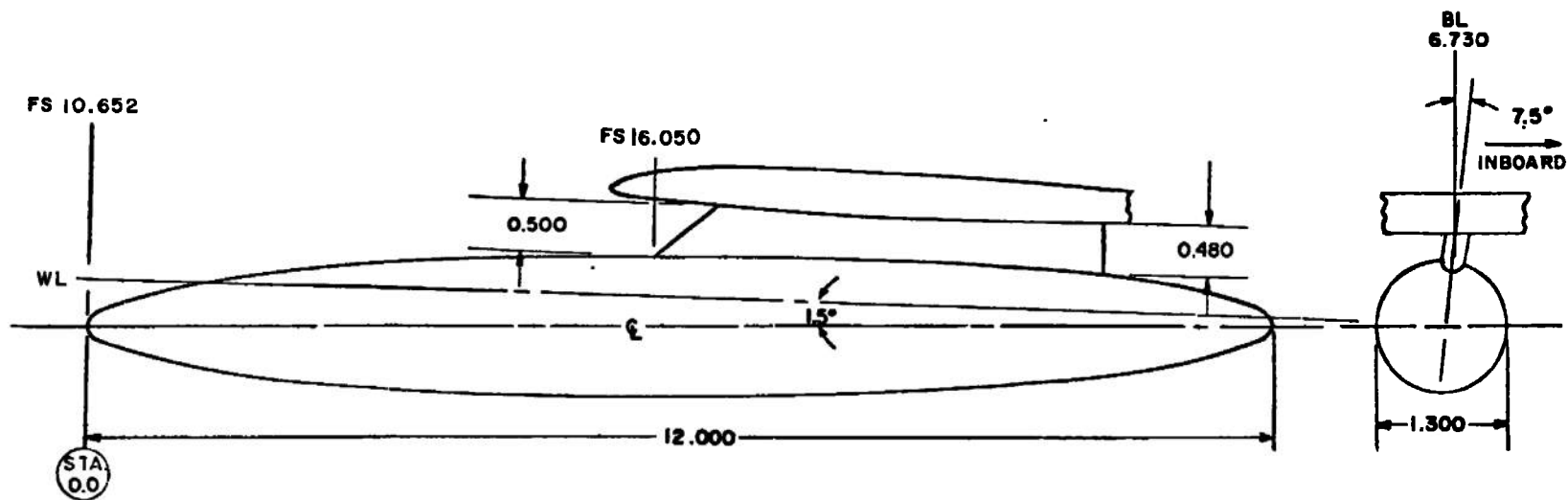
BODY CONTOUR, TYPICAL BOTH ENDS

STATION	BODY DIAM	STATION	BODY DIAM
0.000	0.000	2.500	1.116
0.025	0.100	2.750	1.156
0.050	0.144	3.000	1.190
0.150	0.258	3.250	1.218
0.250	0.340	3.500	1.242
0.500	0.498	3.750	1.260
0.750	0.622	4.000	1.274
1.000	0.724	4.250	1.286
1.250	0.812	4.500	1.294
1.500	0.890	4.750	1.298
1.750	0.958	5.000	1.300
2.000	1.016	6.000	1.300
2.250	1.070		

Fig. 8 Details and Dimensions of the 370-gal Dummy Fuel Tank

BODY CONTOUR

Y	R	Y	R
0 000	0 000	4.250	0 827
0050	0 049	4 500	0.838
0.100	0 077	4.750	0 847
0.150	0.101	5.000	0.854
0.200	0 122	5.250	0.859
0 250	0.143	5 50 0	0 860
0.500	0.232	6.250	0.860
0.750	0.308	6 500	0 859
1.000	0.376	6 750	0 856
1.250	0.438	7 000	0 852
1.500	0.494	7 250	0 846
1.750	0.546	7 500	0.839
2.000	0.593	7.750	0 830
2.250	0.637	8 000	0 820
2.500	0.679	8 250	0.809
2.750	0 713	8.500	0.796
3.000	0.740	8.750	0.781
3.250	0.762	9.000	0.765
3.500	0.782	9.250	0 745
3.750	0.799	13 000	0.400
4.000	0 814		

FUSELAGE STATIONS AND
DIMENSIONS IN INCHES
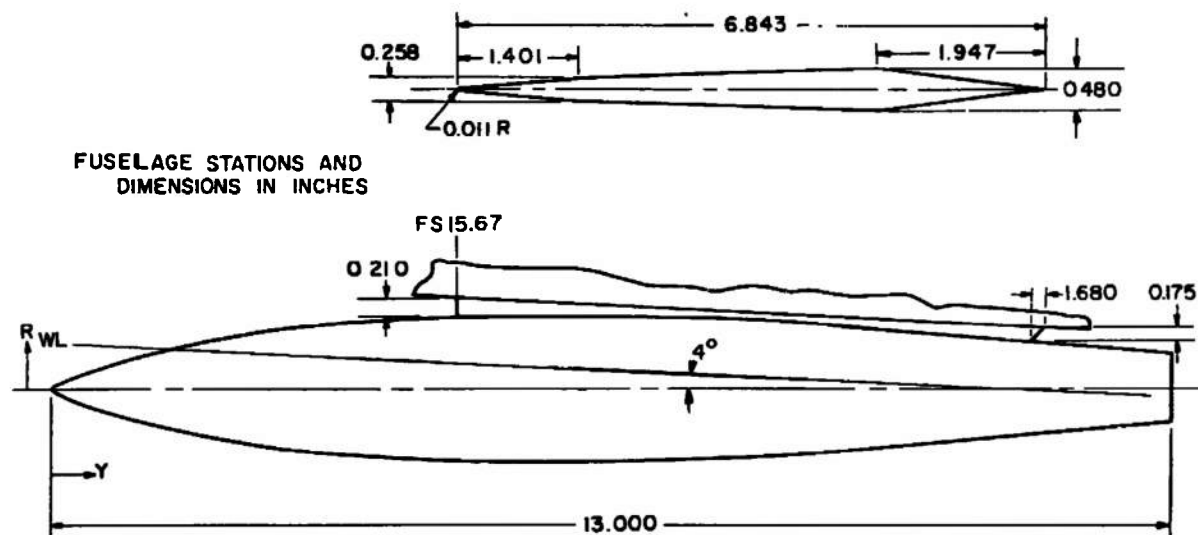
Fig. 9 Details and Dimensions of the 600-gal Dummy Fuel Tank

AEDC
3723-71
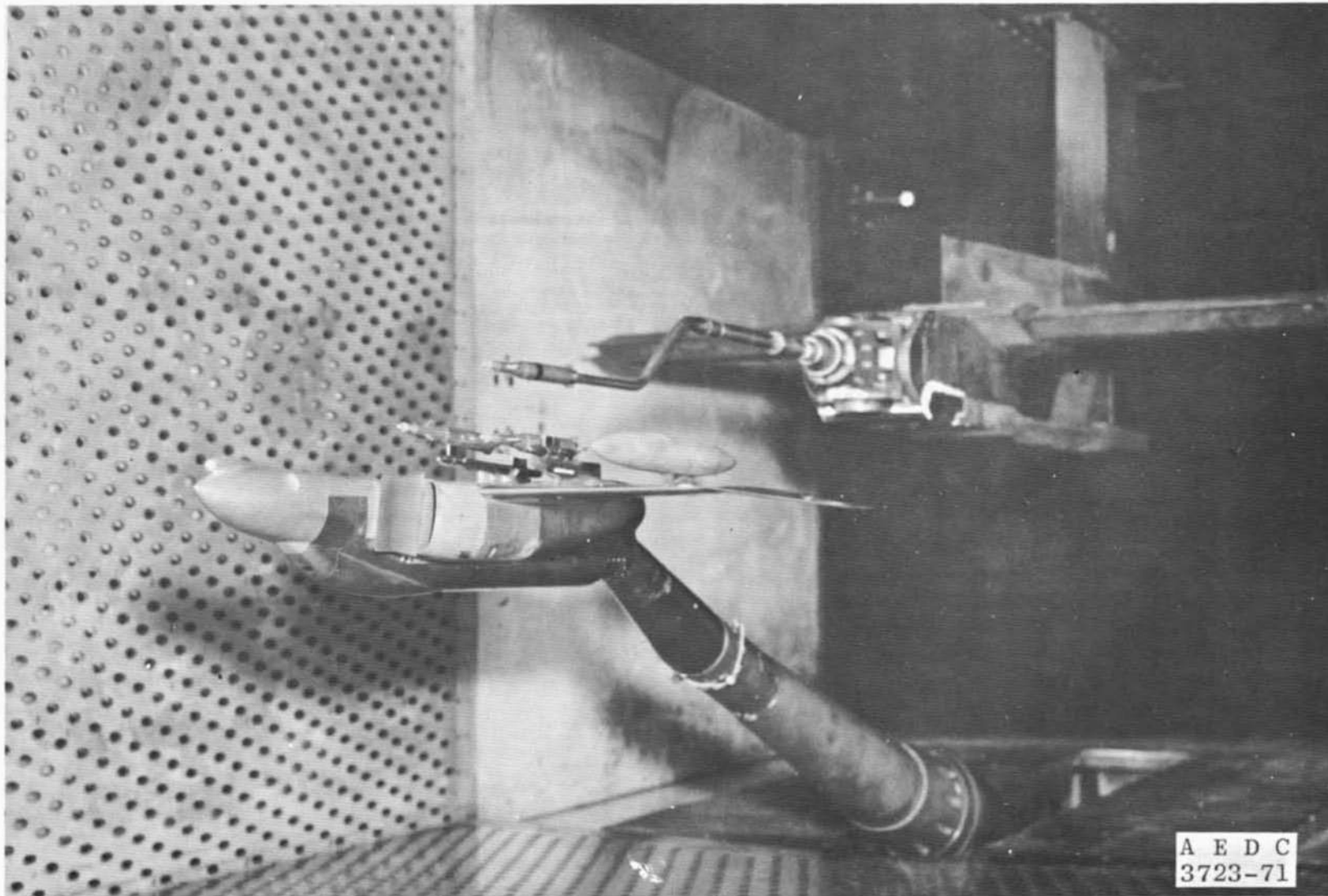
Fig. 10 Tunnel Installation Photograph Showing Parent Aircraft with Stores (Configuration 1) and CTS

AIRCRAFT/WEAPONS LOADING NOMENCLATURE

MER RACK

TER RACK

LOOKING UPSTREAM
F - 4C

RIGHT WING

OUTBOARD PYLON

INB'D PYLON

LAUNCH GRM (LGDM)

DUMMY GRM (LGDM)

DUMMY FUEL TANK

PYLON

MER OR TER RACK

Fig. 11 Aircraft/Weapons Loading Nomenclature

CONFIGURATION 1

RIGHT WING (TYP.)

℄ PYLON	INBOARD PYLON	OUTBOARD PYLON
MER STA.1: EMPTY	TER STA.1: EMPTY	370-GAL. FUEL TANK
MER STA.2: DUMMY	TER STA.2: DUMMY	
MER STA.3: EMPTY	TER STA.3: LAUNCH	
MER STA.4: EMPTY		
MER STA.5: EMPTY		
MER STA.6: EMPTY		

CONFIGURATION 2

℄ PYLON	INBOARD PYLON	OUTBOARD PYLON
MER STA.1: EMPTY	TER STA.1: EMPTY	370-GAL. FUEL TANK
MER STA.2: DUMMY	TER STA.2: LAUNCH	
MER STA.3: EMPTY	TER STA.3: DUMMY	
MER STA.4: EMPTY		
MER STA.5: EMPTY		
MER STA.6: EMPTY		

CONFIGURATION 3

℄ PYLON	INBOARD PYLON	OUTBOARD PYLON
MER STA.1: EMPTY	TER STA.1: EMPTY	370-GAL. FUEL TANK
MER STA.2: DUMMY	TER STA.2: LAUNCH	
MER STA.3: EMPTY	TER STA.3: EMPTY	
MER STA.4: EMPTY		
MER STA.5: DUMMY		
MER STA.6: EMPTY		

CONFIGURATION 4

℄ PYLON	INBOARD PYLON	OUTBOARD PYLON
MER STA.1: EMPTY	TER STA.1: EMPTY	370-GAL. FUEL TANK
MER STA.2: DUMMY	TER STA.2: EMPTY	
MER STA.3: EMPTY	TER STA.3: LAUNCH	
MER STA.4: EMPTY		
MER STA.5: DUMMY		
MER STA.6: EMPTY		

CONFIGURATION 5

℄ PYLON	INBOARD PYLON	OUTBOARD PYLON
600-GAL. FUEL TANK	DUMMY (FIN DEPLOYED)	LAUNCH (FINS DEPLOYED)

CONFIGURATION 6

℄ PYLON	INBOARD PYLON	OUTBOARD PYLON
600-GAL. FUEL TANK	LAUNCH (FINS DEPLOYED)	EMPTY

Fig. 12 Schematic of Aircraft/Weapons Loading Configurations
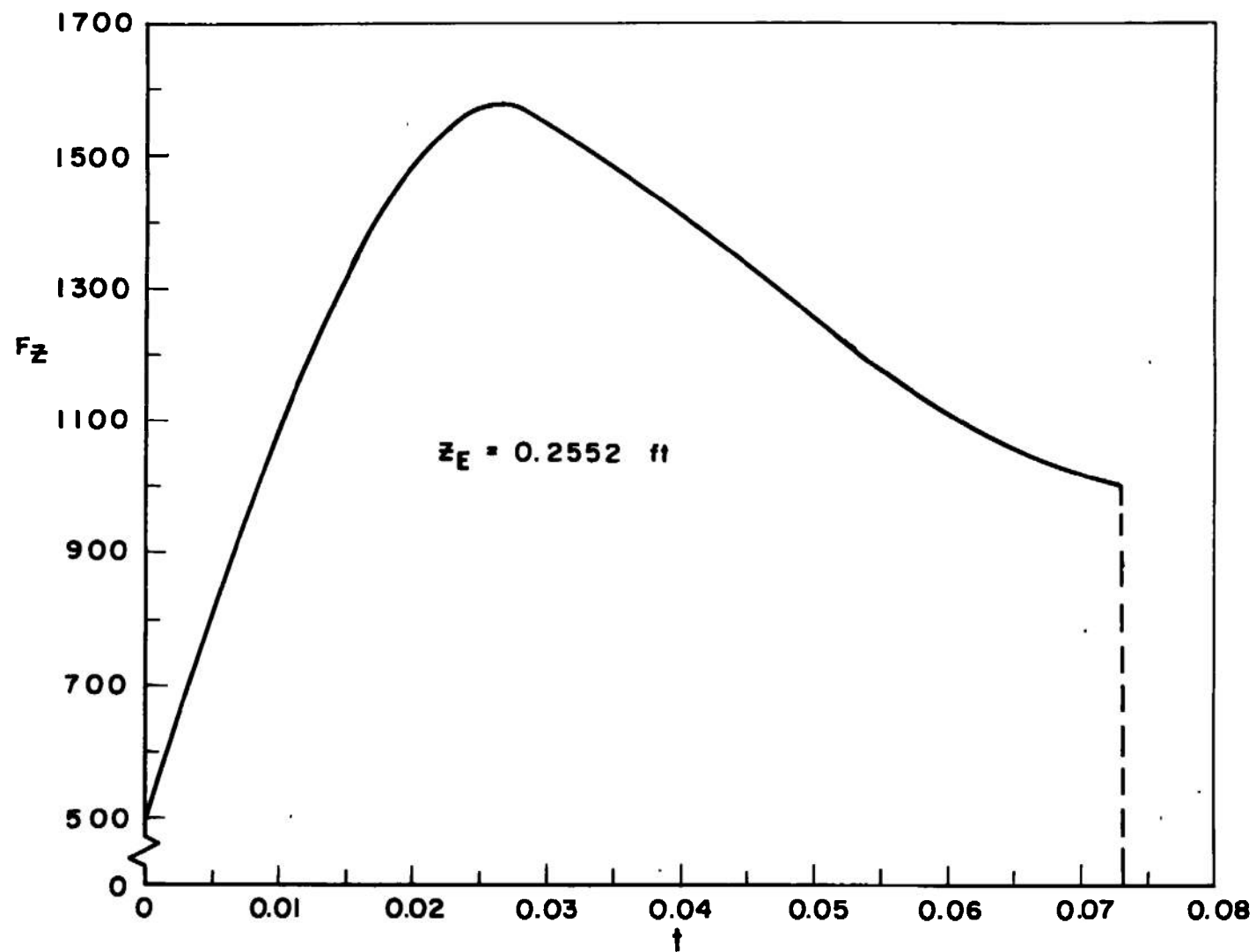
a. TER Ejector Forces
Fig. 13 Ejector Force Functions
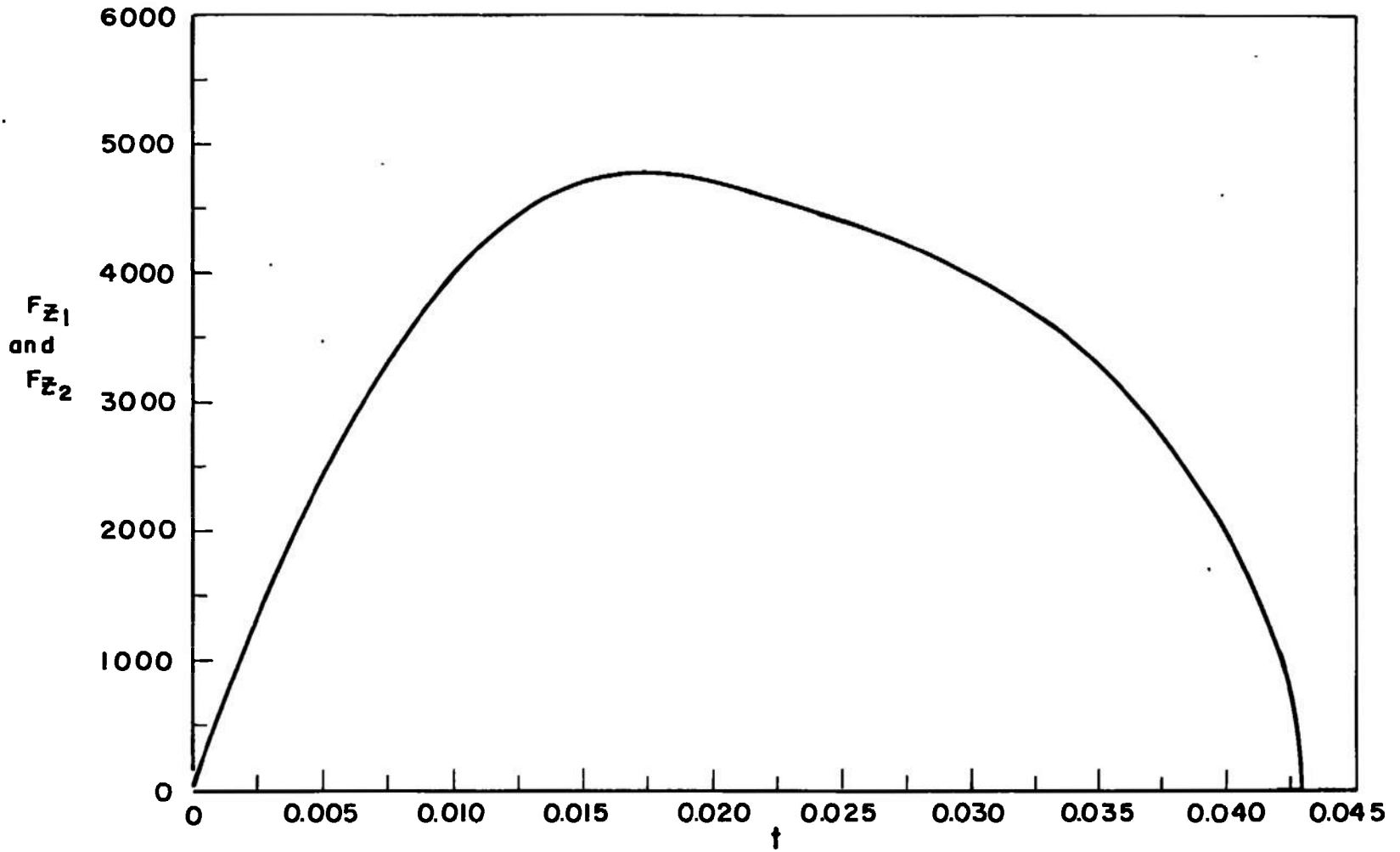
b. Pylon Ejector Forces
Fig. 13 Concluded

SYM	CONF	M_∞	α	H	$\bar\theta$	MOMENT CENTER
◔	1	0.66	1.7	5000	0	N
⊡	1	0.74	1.0	5000	0	N
△	1	0.82	0.5	5000	0	N
◇	1	0.90	0.2	5000	0	N
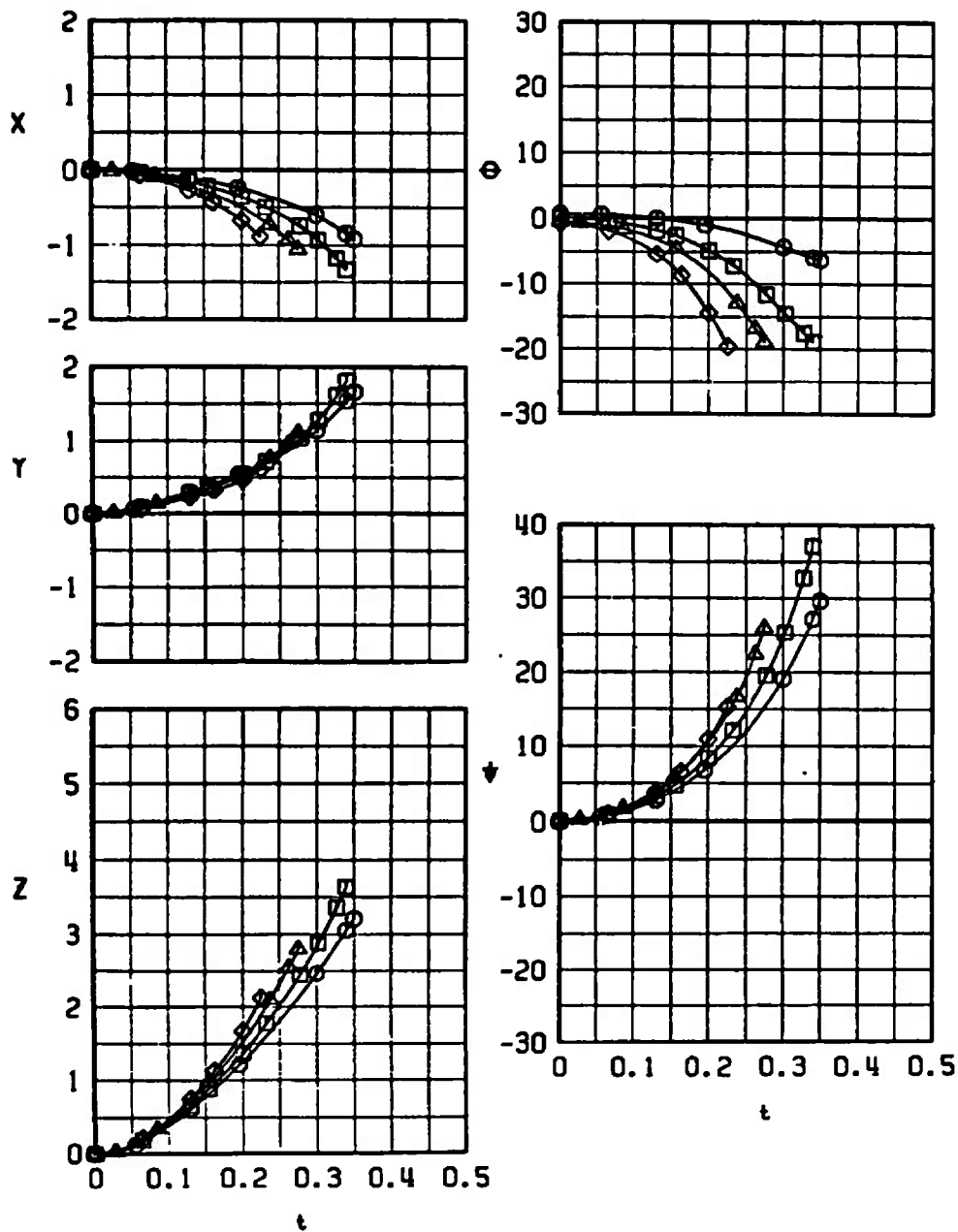
a. Normal Moment Reference, $\bar\theta$ = 0 deg

Fig. 14 Separation Trajectories from Right-Wing TER, Station 3 (Simulated Left-Wing TER, Station 2), Fins Folded

23

SYM	CONF	M_∞	α	H	$\bar{\theta}$	MOMENT CENTER
⊙	1	0.66	0.8	5000	-45	N
⊡	1	0.74	0.4	5000	-45	N
△	1	0.82	0.0	5000	-45	N
◇	1	0.90	-0.2	5000	-45	N
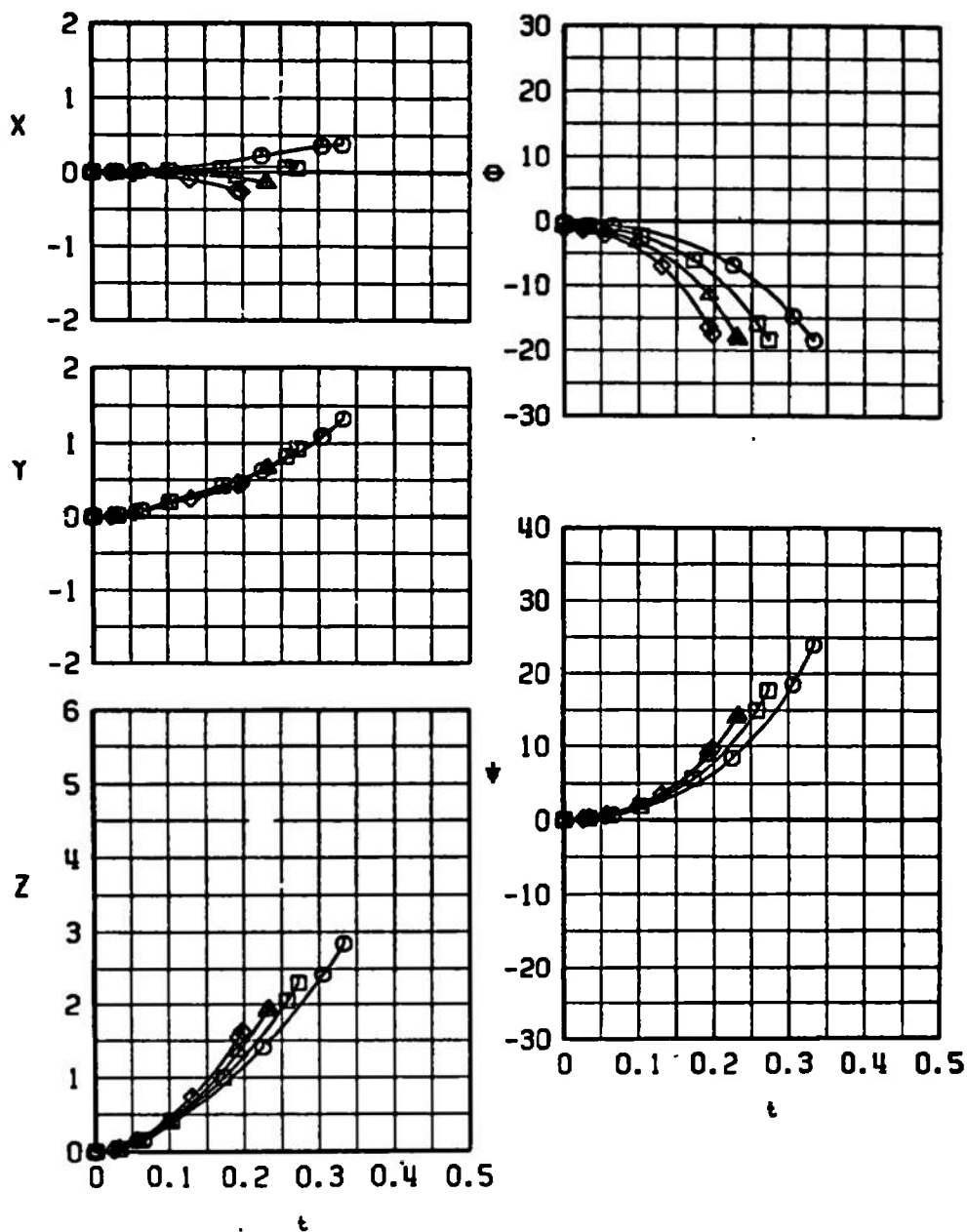
b. Normal Moment Reference, $\bar{\theta}$ = -45 deg
Fig. 14 Continued

24

SYM	CONF	M_∞	α	H	$\bar{\theta}$	MOMENT CENTER
⊙	1	0.66	0.8	5000	-45	F
⊡	1	0.74	0.4	5000	-45	F
△	1	0.82	0.0	5000	-45	F
◇	1	0.90	-0.2	5000	-45	F
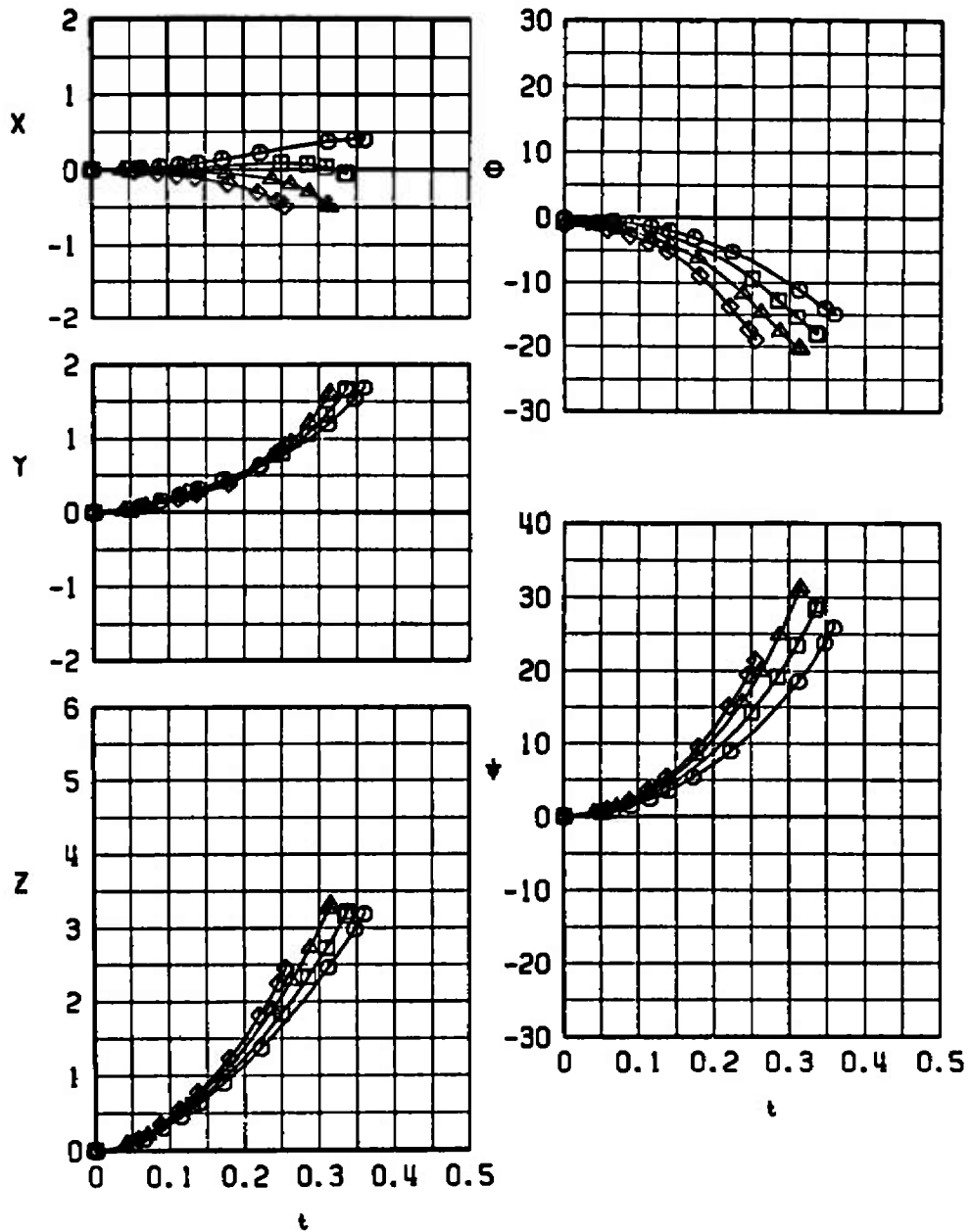
c. Forward Moment Reference, $\bar{\theta}$ = -45 deg

Fig. 14 Concluded

25

SYM	CONF	M_∞	α	H	$\bar{\theta}$	MOMENT CENTER
◐	2	0.66	1.7	5000	0	N
⊡	2	0.74	1.0	5000	0	N
△	2	0.82	0.5	5000	0	N
◇	2	0.90	0.2	5000	0	N
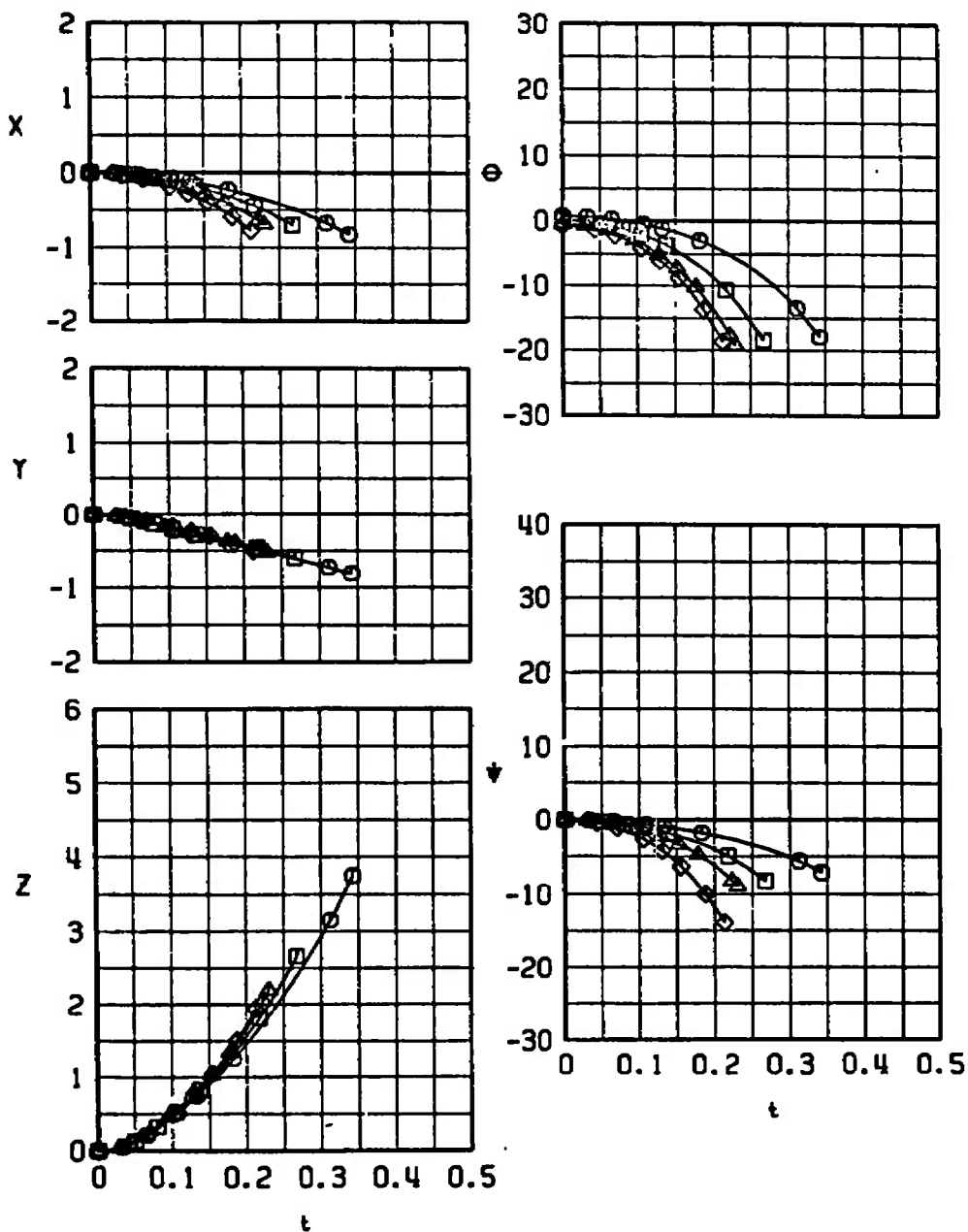
a. Normal Moment Reference, $\bar{\theta}$ = 0 deg

Fig. 15 Separation Trajectories from Right-Wing TER, Station 2, Fins Folded

SYM	CONF	M∞	α	H	θ̄	MOMENT CENTER
◐	2	0.66	0.8	5000	-45	N
⬒	2	0.74	0.4	5000	-45	N
△	2	0.82	0.0	5000	-45	N
◇	2	0.90	-0.2	5000	-45	N
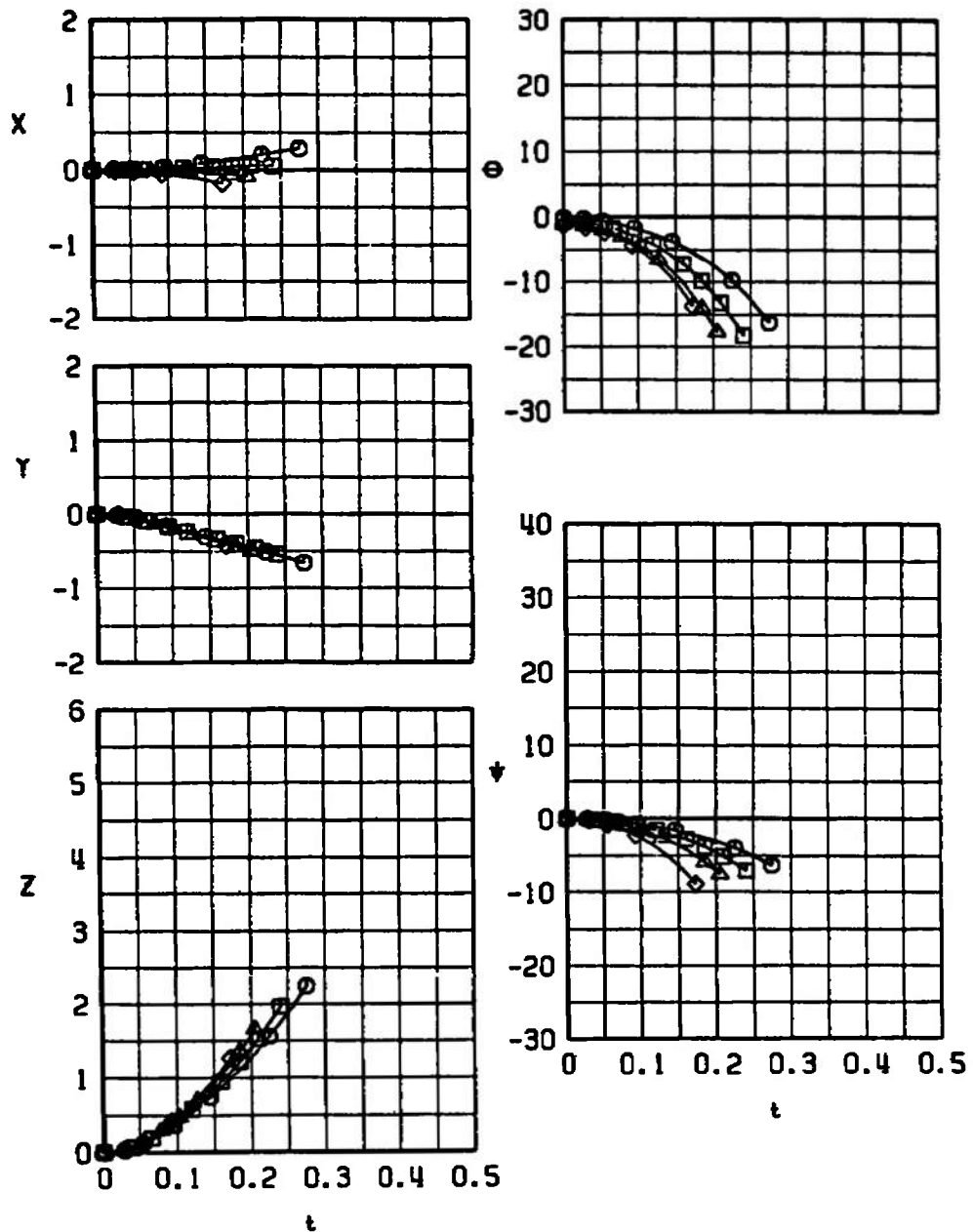
b. Normal Moment Reference, θ̄ = -45 deg
Fig. 15 Continued

SYM	CONF	M_∞	α	H	$\bar\theta$	MOMENT CENTER
⊙	2	0.66	0.8	5000	-45	F
▫	2	0.74	0.4	5000	-45	F
△	2	0.82	0.0	5000	-45	F
◇	2	0.90	-0.2	5000	-45	F
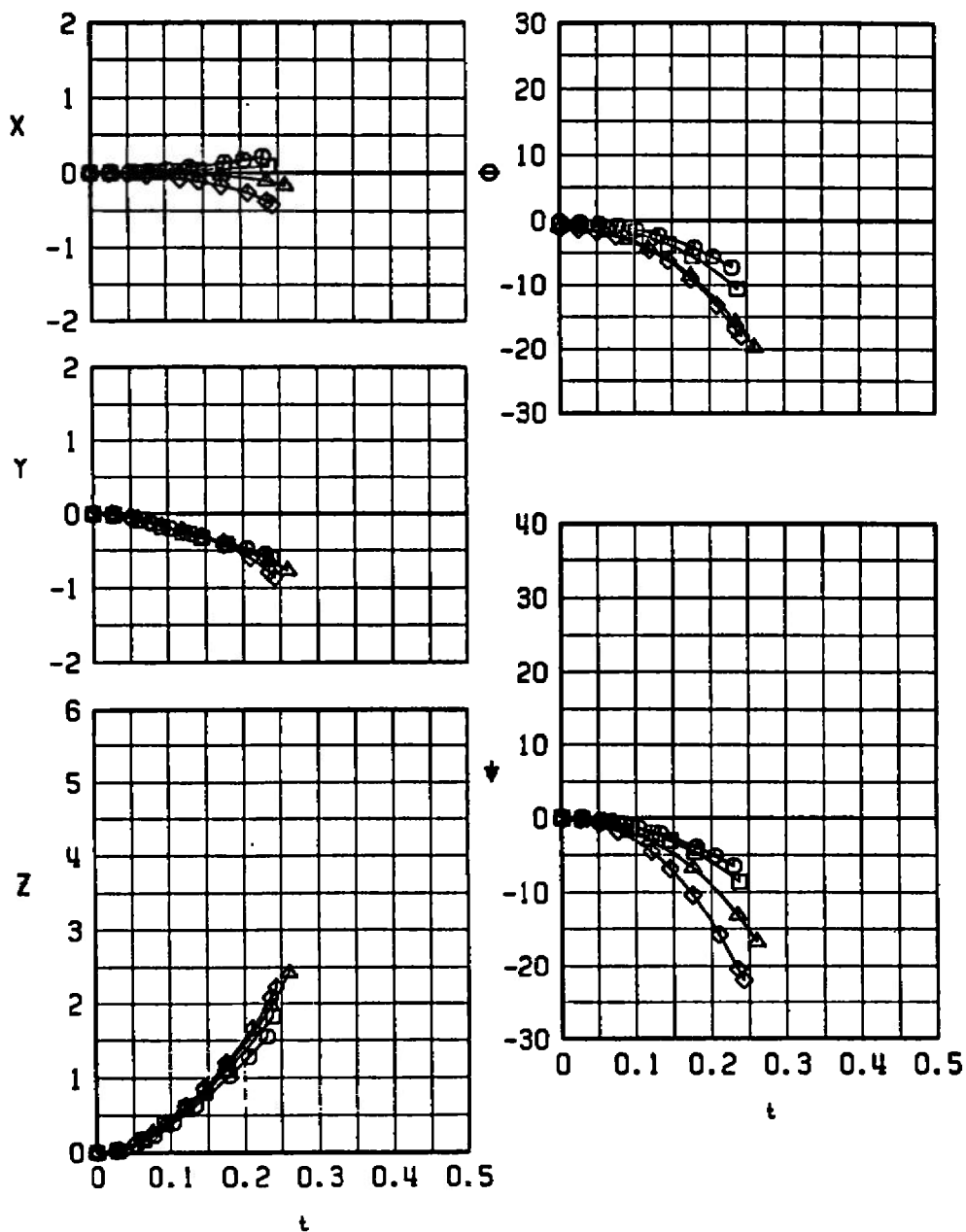
c. Forward Moment Reference, $\bar\theta$ = -45 deg

Fig. 15 Concluded

28

SYM	CONF	M_∞	α	H	$\bar{\theta}$	MOMENT CENTER
◐	3	0.66	1.7	5000	0	N
⊡	3	0.74	1.0	5000	0	N
△	3	0.82	0.5	5000	0	N
◇	3	0.90	0.2	5000	0	N
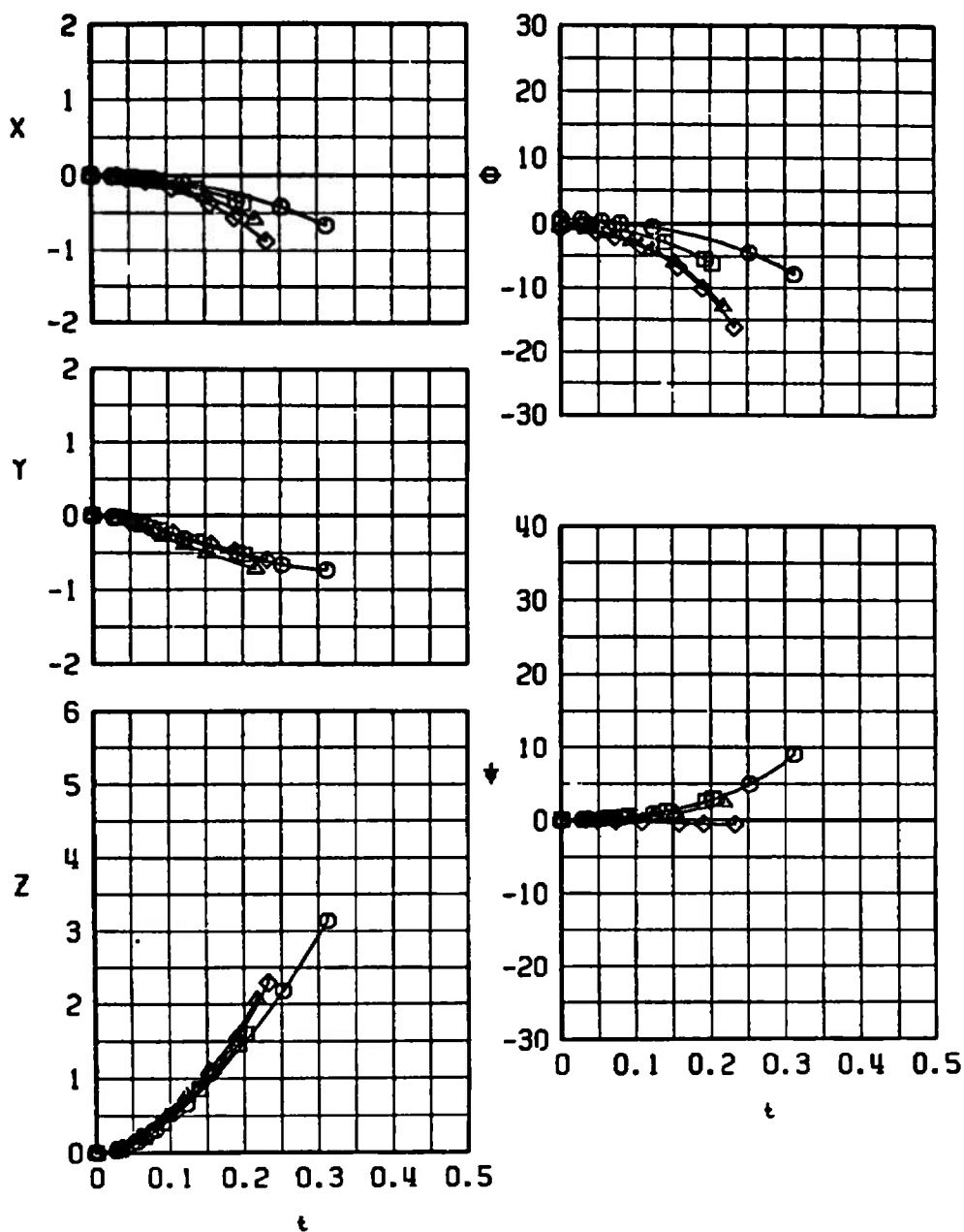
a. Normal Moment Reference, $\bar{\theta}$ = 0 deg

Fig. 16 Separation Trajectories from Right-Wing TER, Station 2 (Simulated Left-Wing TER, Station 3), Fins Folded

SYM	CONF	M_∞	α	H	$\bar{\theta}$	MOMENT CENTER
⊙	3	0.66	0.8	5000	-45	N
⊡	3	0.74	0.4	5000	-45	N
△	3	0.82	0.0	5000	-45	N
◇	3	0.90	-0.2	5000	-45	N
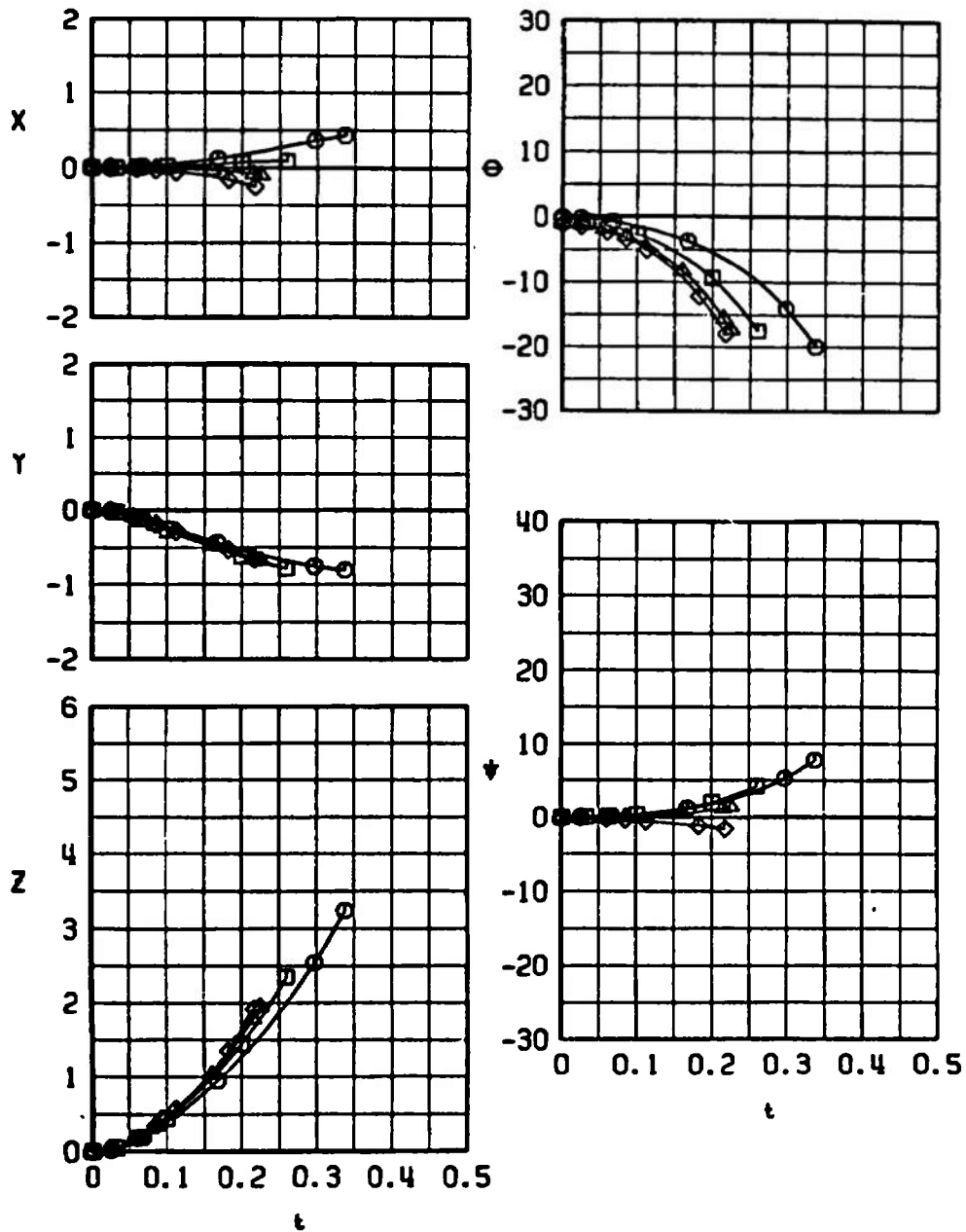
b. Normal Moment Reference, $\bar{\theta}$ = -45 deg
Fig. 16 Continued

30

SYM	CONF	M_∞	α	H	$\bar{\theta}$	MOMENT CENTER
◯	3	0.66	0.8	5000	-45	F
◻	3	0.74	0.4	5000	-45	F
△	3	0.82	0.0	5000	-45	F
◇	3	0.90	-0.2	5000	-45	F
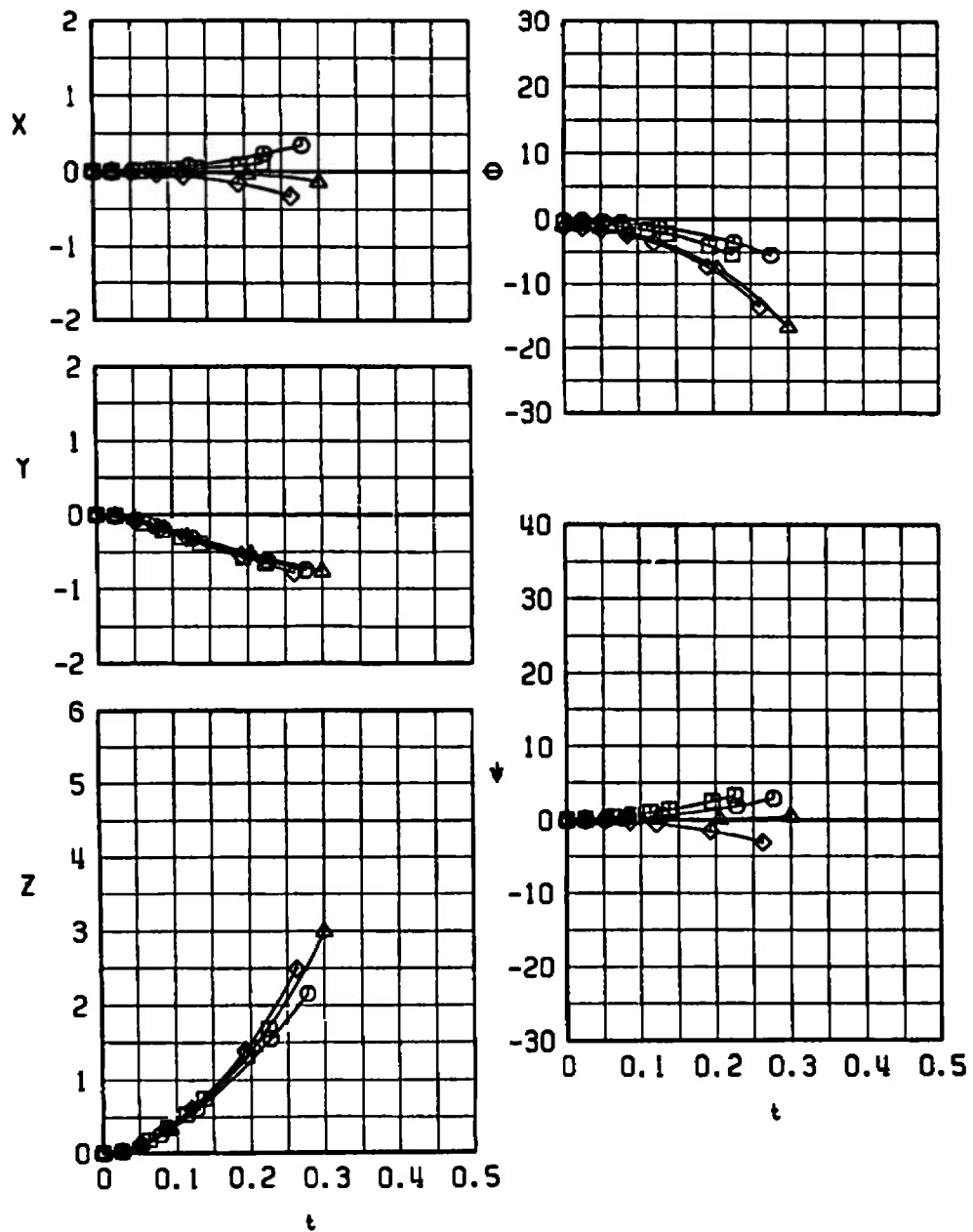
c. Forward Moment Reference, $\bar{\theta}$ = -45 deg

Fig. 16 Concluded

31

SYM	CONF	M_∞	α	H	$\bar{\theta}$	MOMENT CENTER
⊙	4	0.66	1.7	5000	0	N
⊡	4	0.74	1.0	5000	0	N
△	4	0.82	0.5	5000	0	N
◇	4	0.90	0.2	5000	0	N
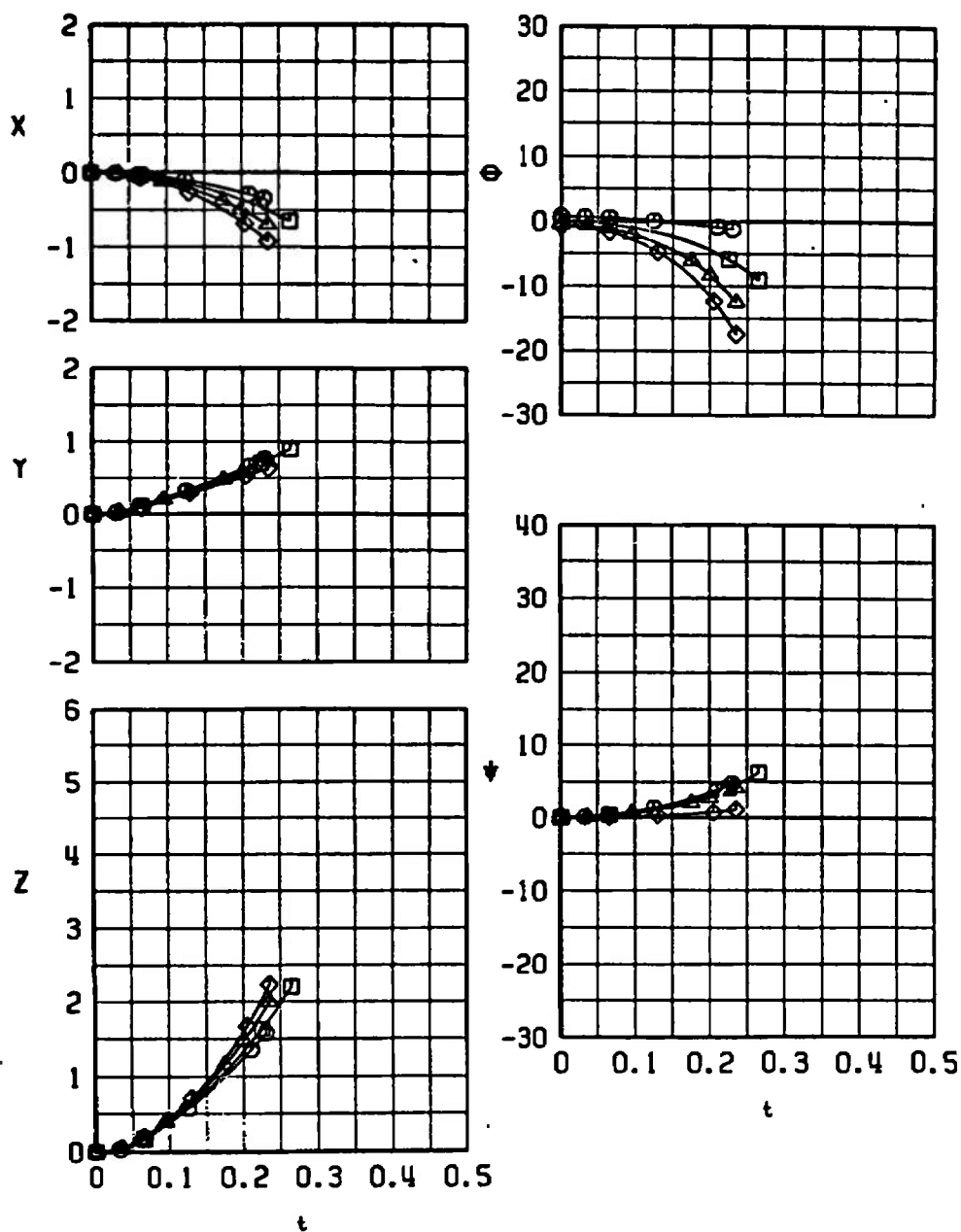
a. Normal Moment Reference, $\bar{\theta}$ = 0 deg

Fig. 17 Separation Trajectories from Right-Wing TER, Station 3, Fins Folded

32

SYM	CONF	M_∞	α	H	$\bar{\theta}$	MOMENT CENTER
☉	4	0.66	0.8	5000	-45	N
▫	4	0.74	0.4	5000	-45	N
△	4	0.82	0.0	5000	-45	N
◇	4	0.90	-0.2	5000	-45	N
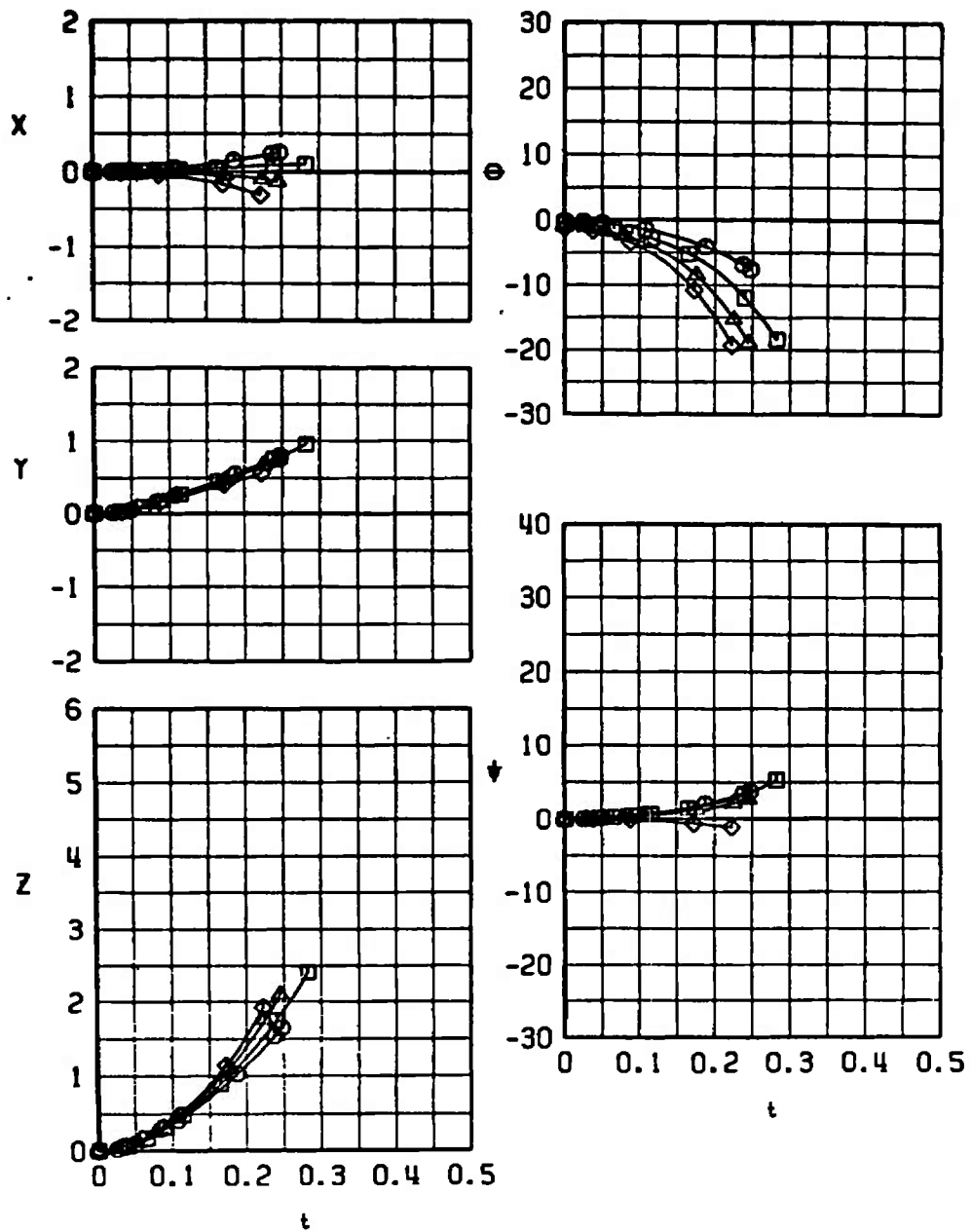
b. Normal Moment Reference, $\bar{\theta}$ = -45 deg

Fig. 17 Continued

SYM	CONF	M_∞	α	H	$\bar{\theta}$	MOMENT CENTER
⊙	4	0.66	0.8	5000	-45	F
▢	4	0.74	0.4	5000	-45	F
△	4	0.82	0.0	5000	-45	F
◇	4	0.90	-0.2	5000	-45	F
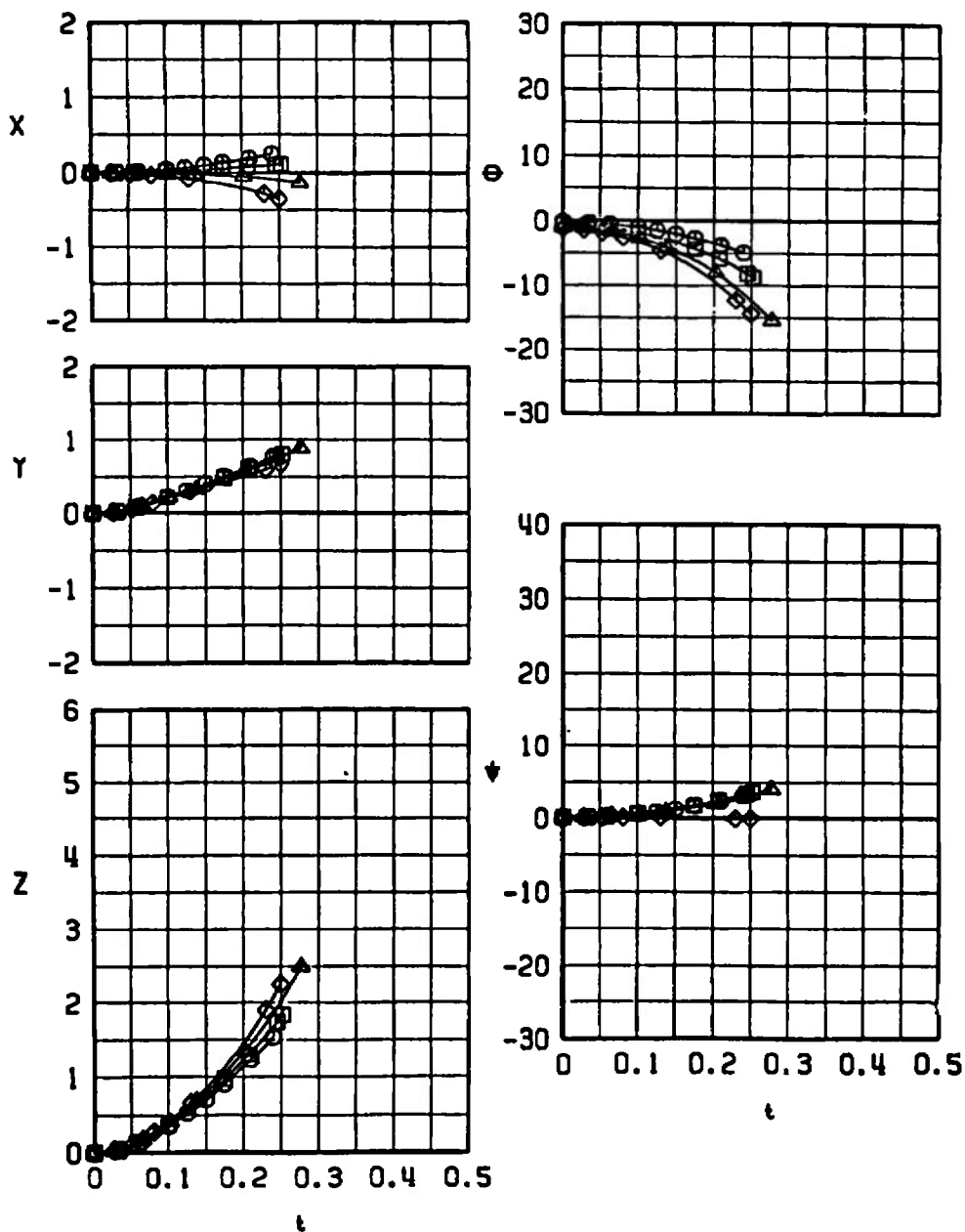
c. Forward Moment Reference, $\bar{\theta}$ = -45 deg

Fig. 17 Concluded

34

SYM	CONF	M_∞	α	H	$\bar{\theta}$	MOMENT CENTER	FINS
⊙	1	0.66	1.7	5000	0	N	FOLDED
△	1	0.66	1.7	5000	0	N	OPEN
⊡	1	0.74	1.0	5000	0	N	FOLDED
◇	1	0.74	1.0	5000	0	N	OPEN
◁	1	0.82	0.5	5000	0	N	FOLDED
▷	1	0.82	0.5	5000	0	N	OPEN
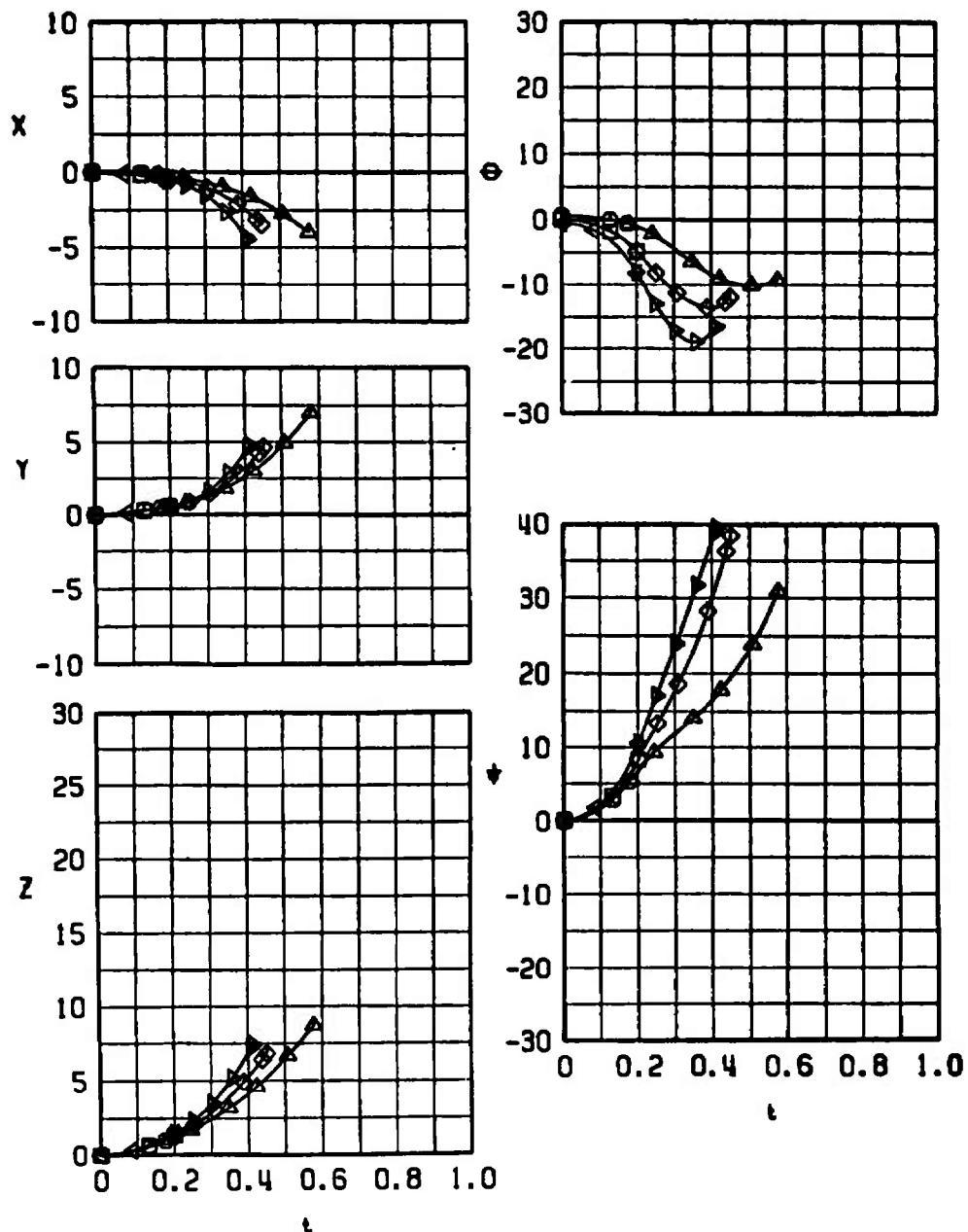
a. Normal Moment Reference, $\bar{\theta}$ = 0 deg

Fig. 18 Effect of Open Fins on the Separation Trajectories from the Right-Wing TER, Station 3 (Simulated Left-Wing TER, Station 2)

35

SYM	CONF	M_∞	α	H	$\bar{\theta}$	MOMENT CENTER	FINS
⊙	1	0.66	0.8	5000	-45	N	FOLDED
▢	1	0.66	0.8	5000	-45	N	OPEN
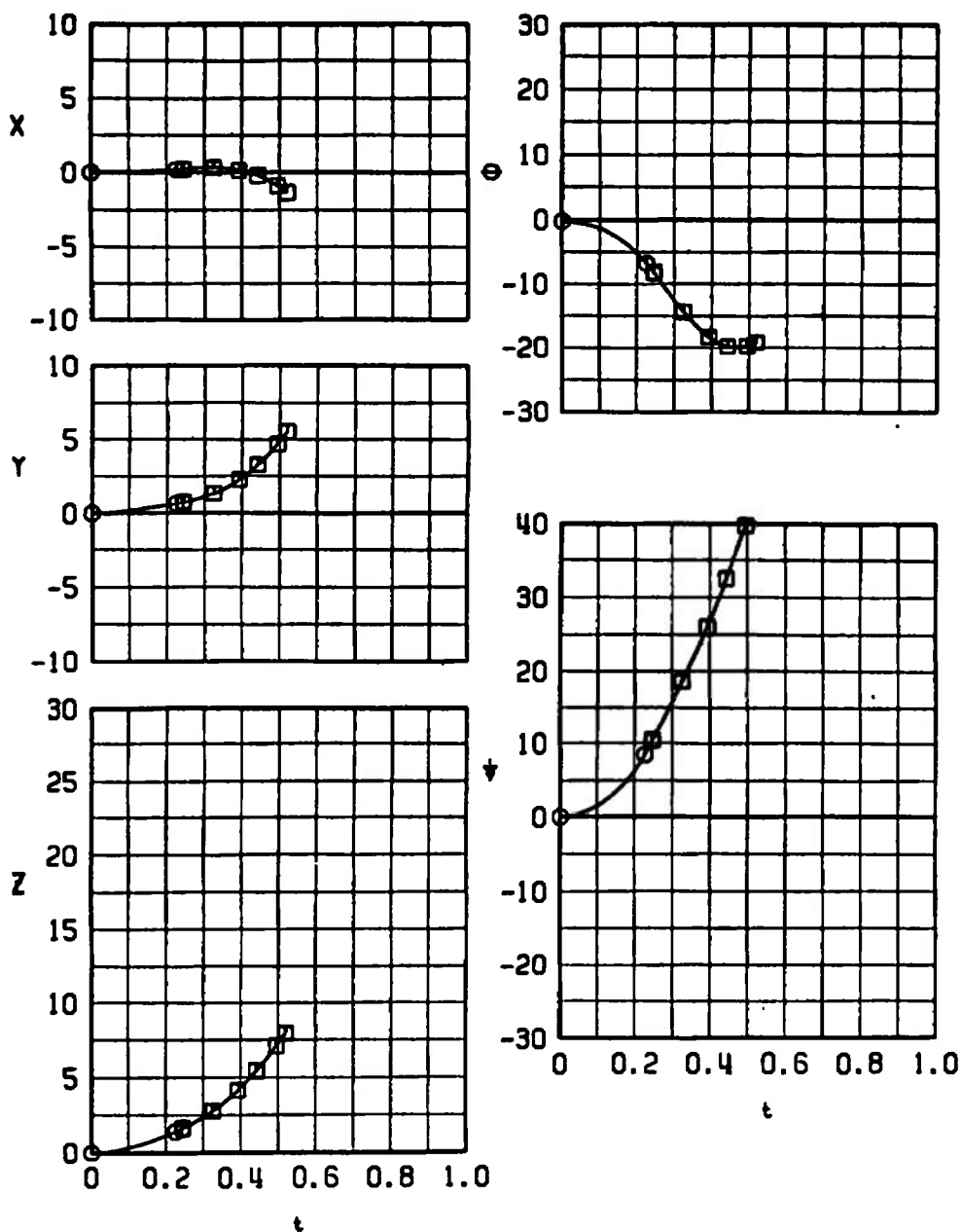
b. Normal Moment Reference, $\bar{\theta}$ = -45 deg

Fig. 18 Continued

SYM	CONF	M∞	α	H	θ̄	MOMENT CENTER	FINS
⊙	1	0.66	0.8	5000	-45	F	FOLDED
△	1	0.66	0.8	5000	-45	F	OPEN
⊡	1	0.74	0.4	5000	-45	F	FOLDED
◇	1	0.74	0.4	5000	-45	F	OPEN
◁	1	0.82	0.0	5000	-45	F	FOLDED
▷	1	0.82	0.0	5000	-45	F	OPEN
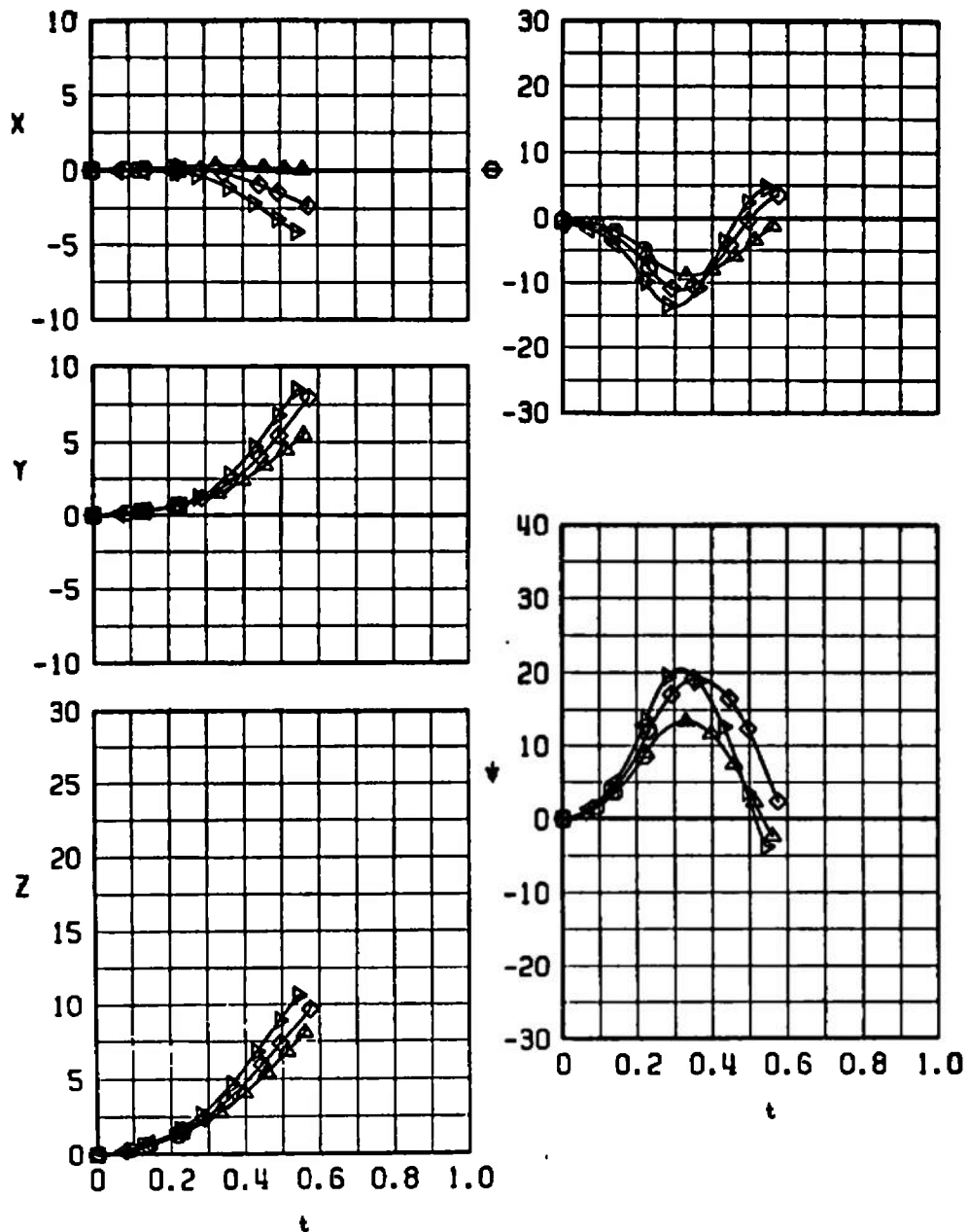
c. Forward Moment Reference, θ̄ = -45 deg

Fig. 18 Concluded

37

SYM	CONF	M_∞	α	H	$\bar{\theta}$	MOMENT CENTER	FINS
⊖	2	0.66	1.7	5000	0	N	FOLDED
▲	2	0.66	1.7	5000	0	N	OPEN
▣	2	0.74	1.0	5000	0	N	FOLDED
◇	2	0.74	1.0	5000	0	N	OPEN
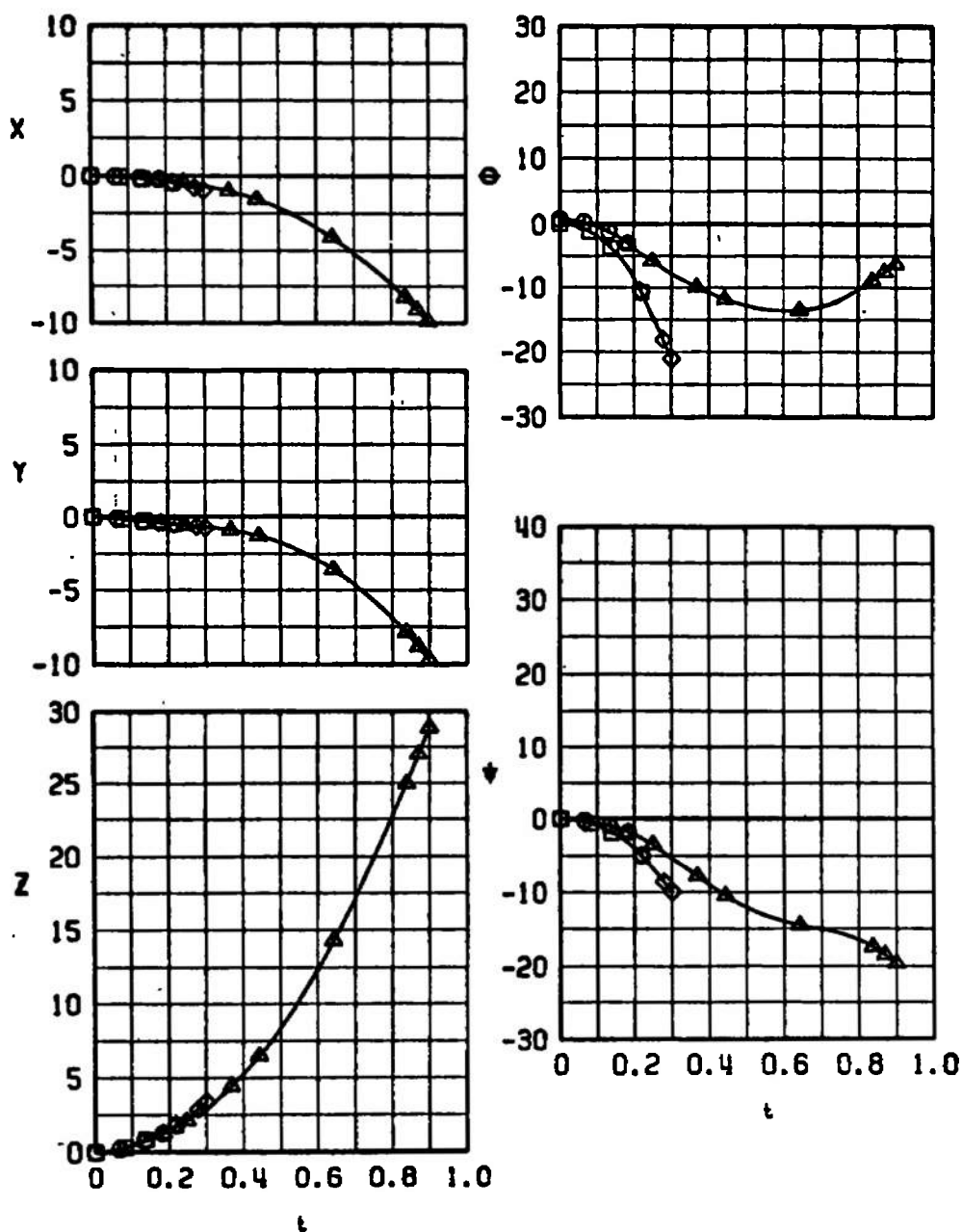
a. Normal Moment Reference, $\bar{\theta}$ = 0 deg

Fig. 19 Effect of Open Fins on the Separation Trajectories from the Right-Wing TER, Station 2

SYM	CONF	M_∞	α	H	$\bar{\theta}$	MOMENT CENTER	FINS
☉	2	0.66	0.8	5000	-45	F	FOLDED
△	2	0.66	0.8	5000	-45	F	OPEN
⊡	2	0.74	0.4	5000	-45	F	FOLDED
◇	2	0.74	0.4	5000	-45	F	OPEN
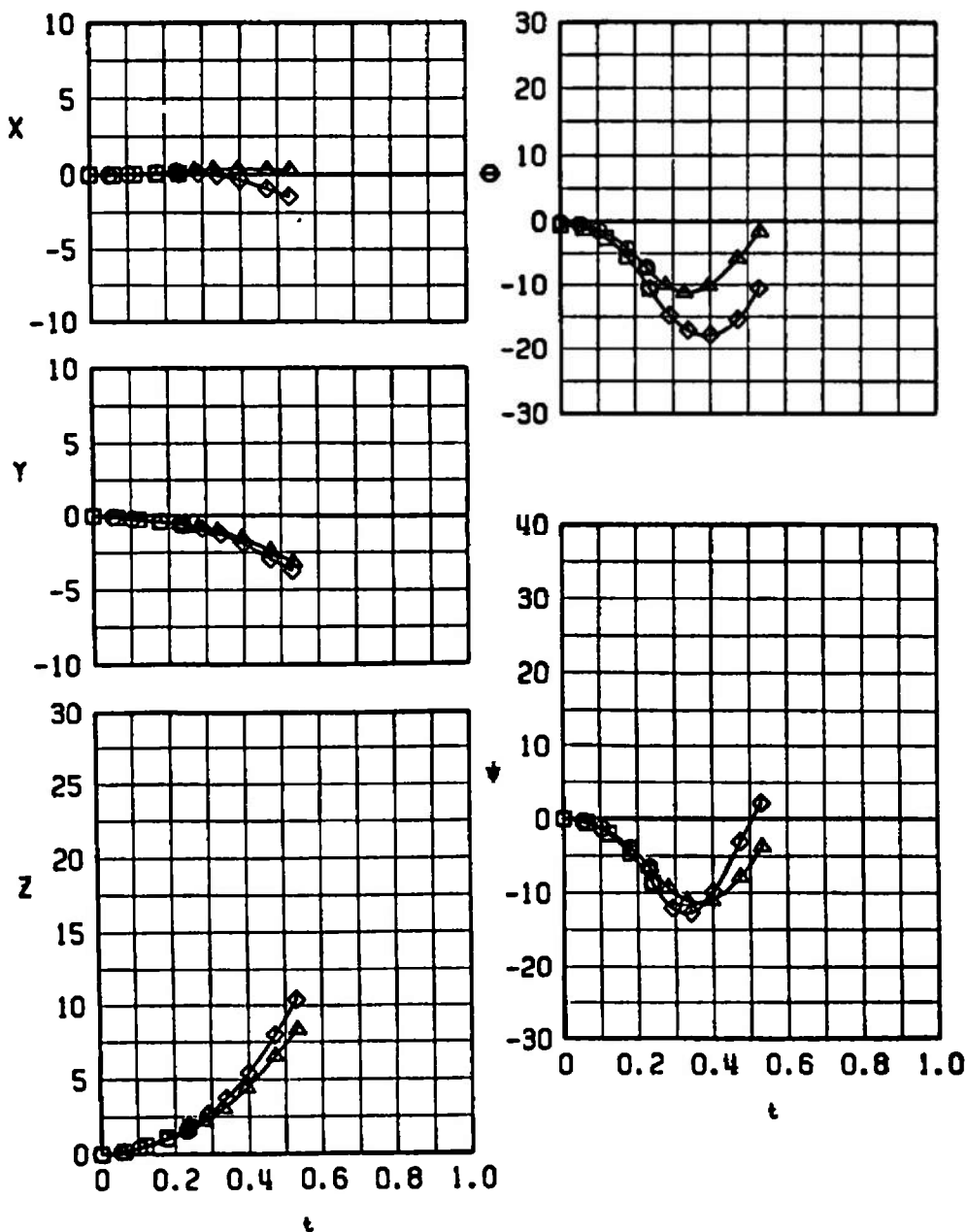
b. Forward Moment Reference, $\bar{\theta}$ = -45 deg
Fig. 19 Concluded

SYM	CONF	M∞	∝	H	$\bar{\theta}$	MOMENT CENTER	FINS
○	3	0.66	1.7	5000	0	N	FOLDED
△	3	0.66	1.7	5000	0	N	OPEN
⊡	3	0.74	1.0	5000	0	N	FOLDED
◇	3	0.74	1.0	5000	0	N	OPEN
◁	3	0.82	0.5	5000	0	N	FOLDED
▷	3	0.82	0.5	5000	0	N	OPEN
▽	3	0.90	0.2	5000	0	N	FOLDED
⊠	3	0.90	0.2	5000	0	N	OPEN
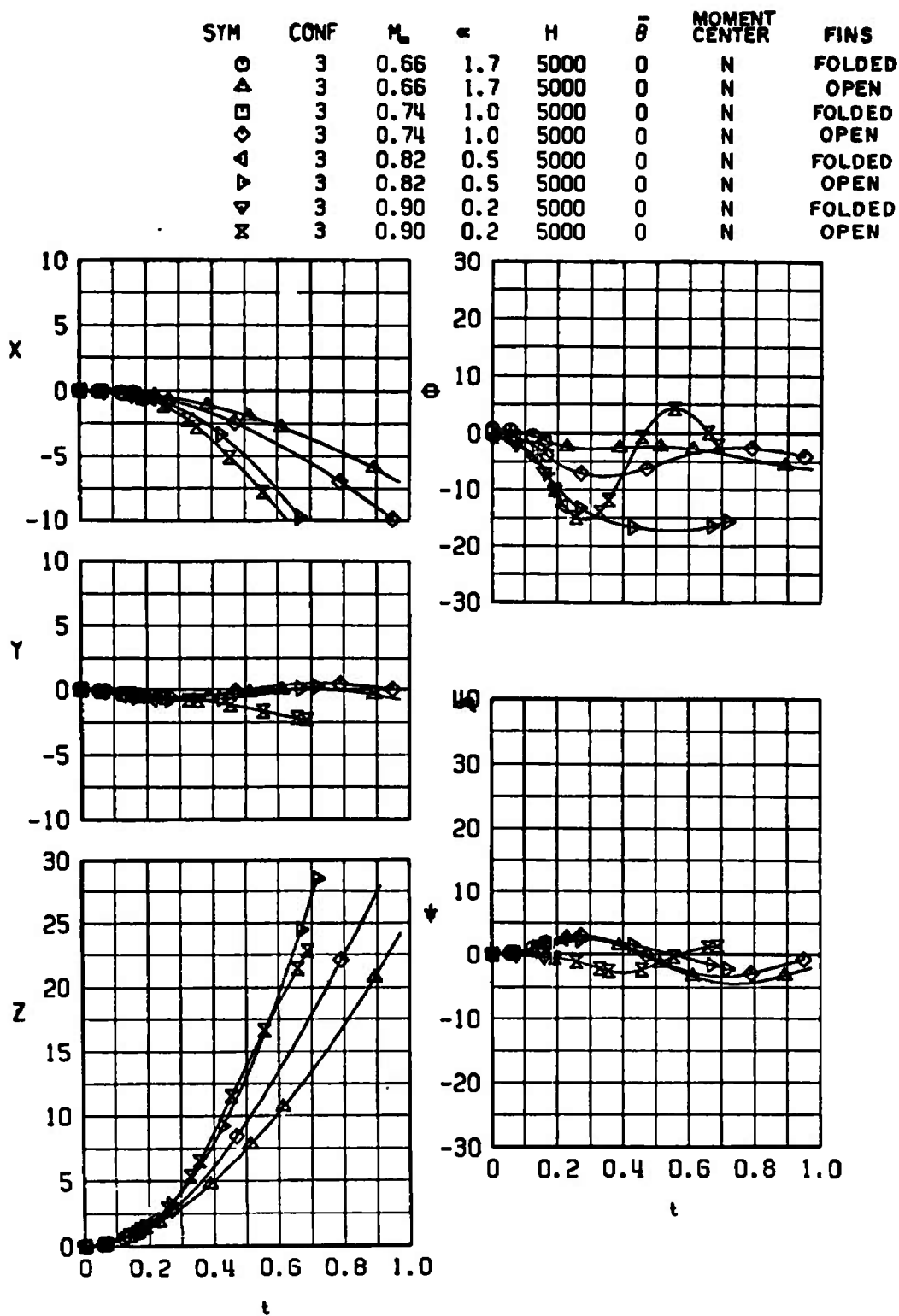
a. Normal Moment Reference, $\bar{\theta}$ = 0 deg

Fig. 20 Effect of Open Fins on the Separation Trajectories from the Right-Wing TER, Station 2 (Simulated Left-Wing TER, Station 3)

40

SYM	CONF	M_∞	α	H	$\bar{\theta}$	MOMENT CENTER	FINS
⊙	3	0.66	0.8	5000	-45	N	FOLDED
⊡	3	0.66	0.8	5000	-45	N	OPEN

b. Normal Moment Reference, $\bar{\theta}$ = -45 deg
Fig. 20 Concluded

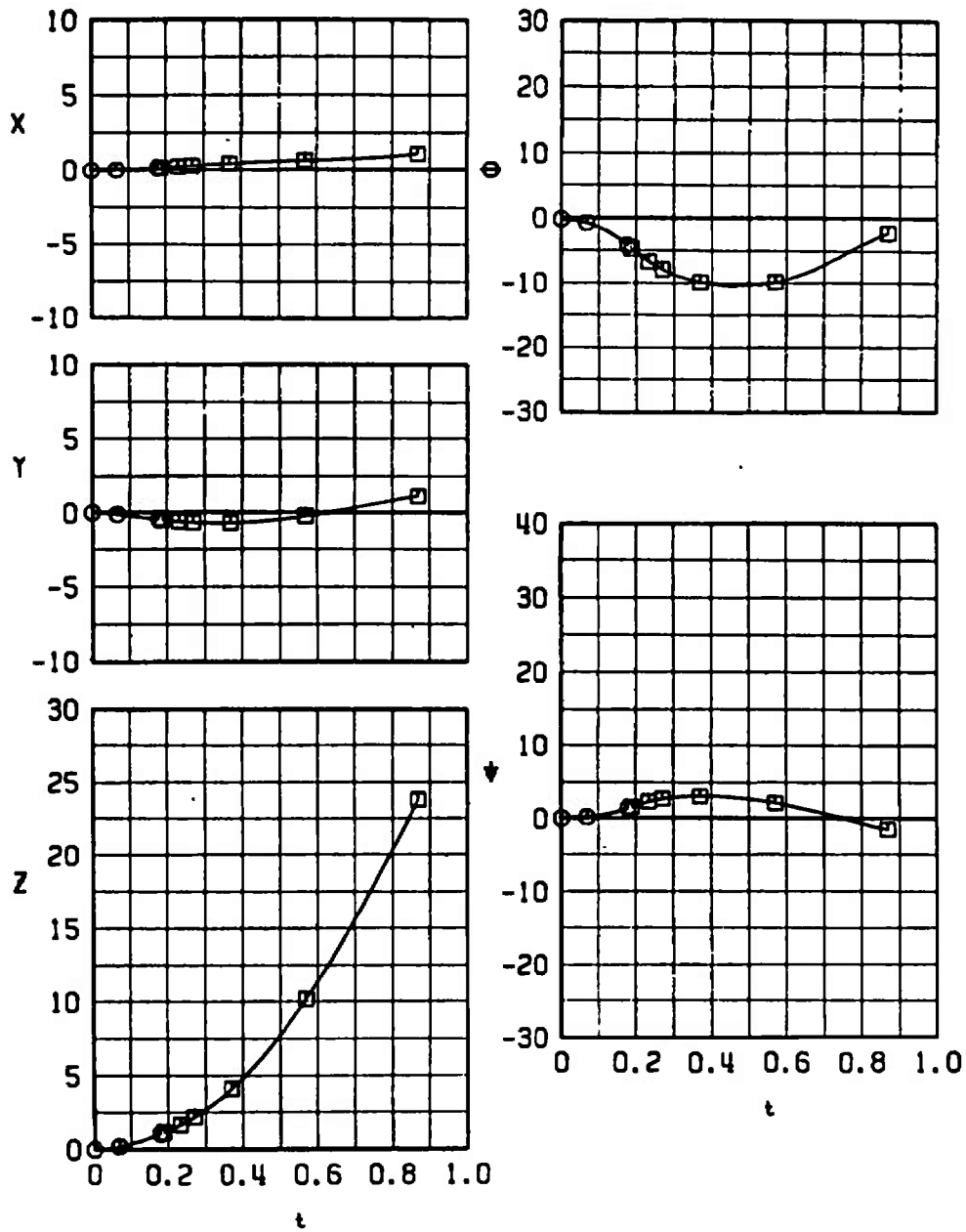| SYM	CONF	M_∞	α	H	$\bar\theta$	MOMENT CENTER	FINS
☉	4	0.66	1.7	5000	0	N	FOLDED
△	4	0.66	1.7	5000	0	N	OPEN
⊡	4	0.74	1.0	5000	0	N	FOLDED
◇	4	0.74	1.0	5000	0	N	OPEN
◁	4	0.82	0.5	5000	0	N	FOLDED
▷	4	0.82	0.5	5000	0	N	OPEN
▽	4	0.90	0.2	5000	0	N	FOLDED
☒	4	0.90	0.2	5000	0	N	OPEN
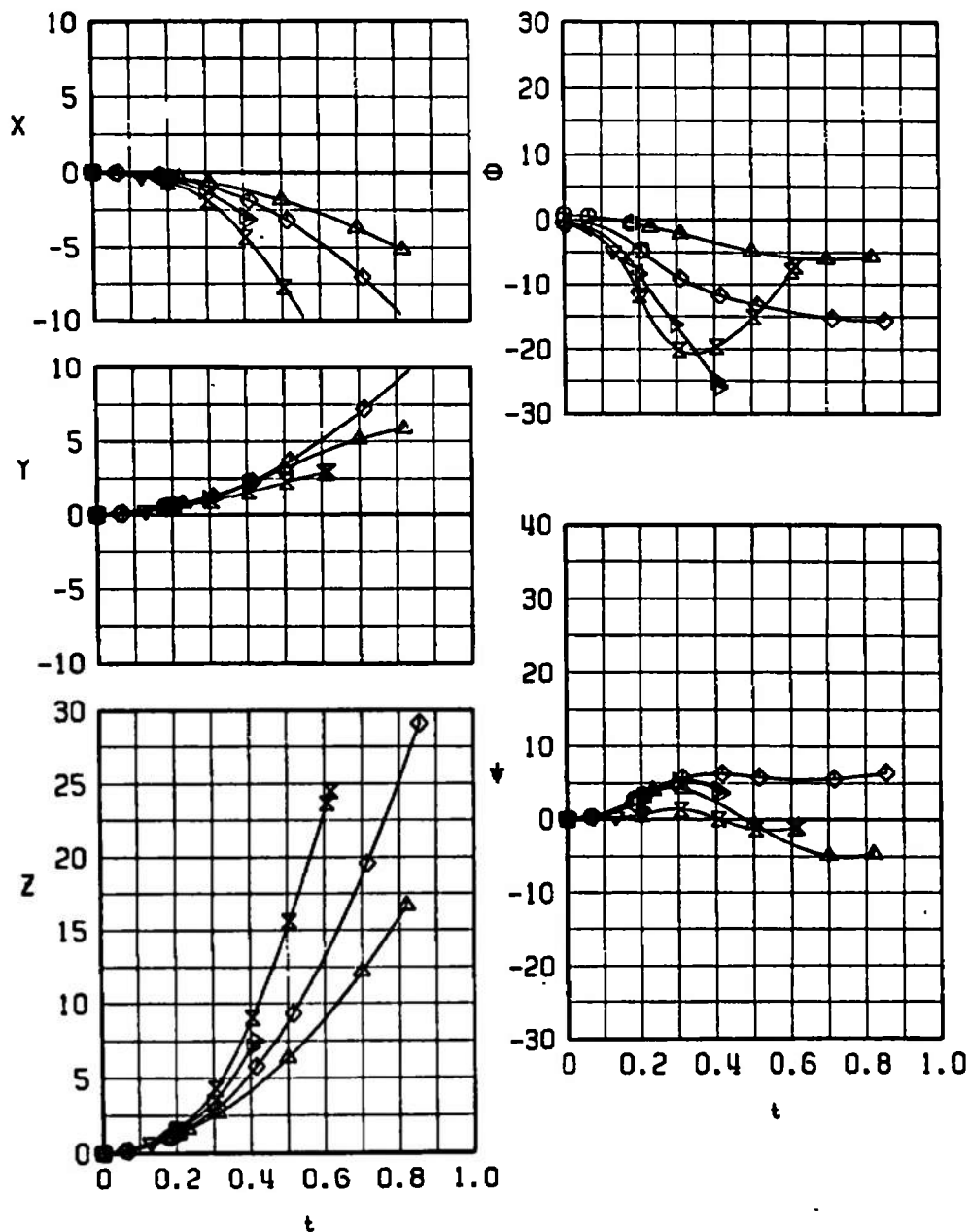
a. Normal Moment Reference, $\bar\theta$ = 0 deg

Fig. 21 Effect of Open Fins on the Separation Trajectories from the Right-Wing TER, Station 3

42

SYM	CONF	M∞	∝	H	$\bar{\theta}$	MOMENT CENTER	FINS
⊙	4	0.66	0.8	5000	-45	N	FOLDED
▢	4	0.66	0.8	5000	-45	N	OPEN
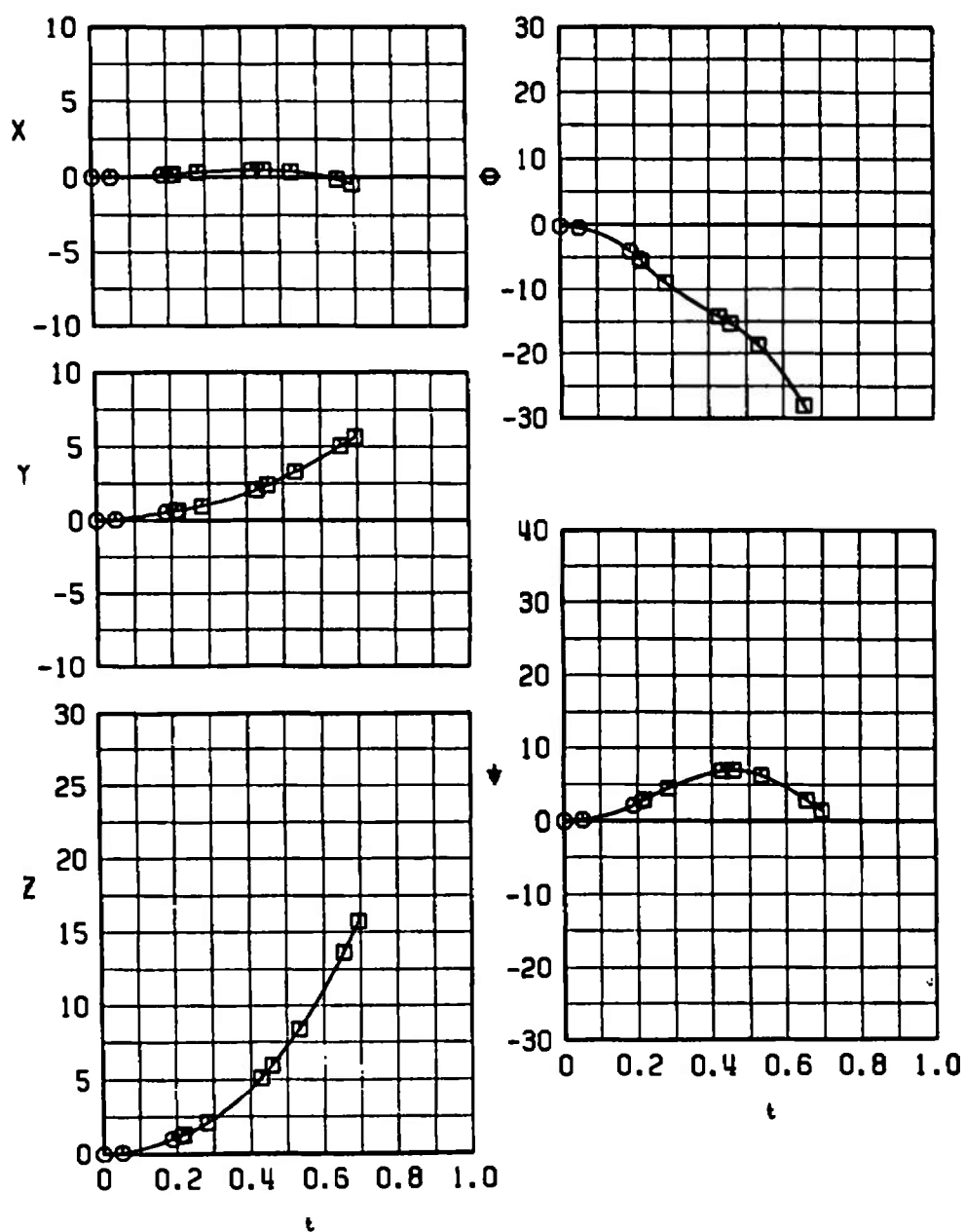
b. Normal Moment Reference, $\bar{\theta}$ = -45 deg
Fig. 21 Concluded

SYM	CONF	M∞	α	H	θ̄
○	5	0.66	1.7	5000	0
□	5	0.74	1.0	5000	0
△	5	0.82	0.5	5000	0
◇	5	0.90	0.2	5000	0
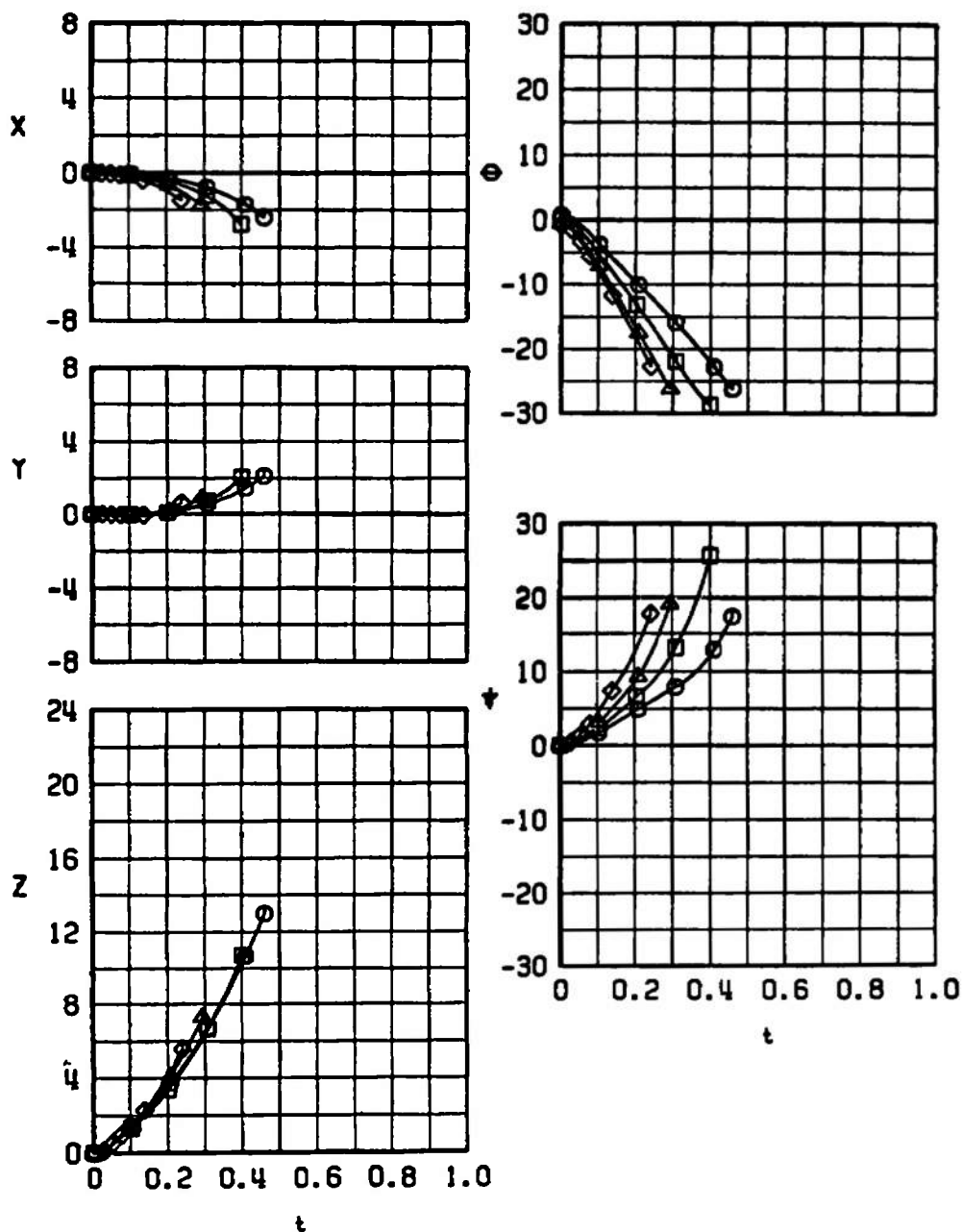
a. θ̄ = 0 deg

Fig. 22 Separation Trajectories from Right-Wing Outboard Pylon;
Fins Deployed

44

STM	CONF	M∞	α	H	δ̄
⊙	5	0.66	0.8	5000	-45
⊡	5	0.74	0.4	5000	-45
△	5	0.82	0.0	5000	-45
◇	5	0.90	-0.2	5000	-45
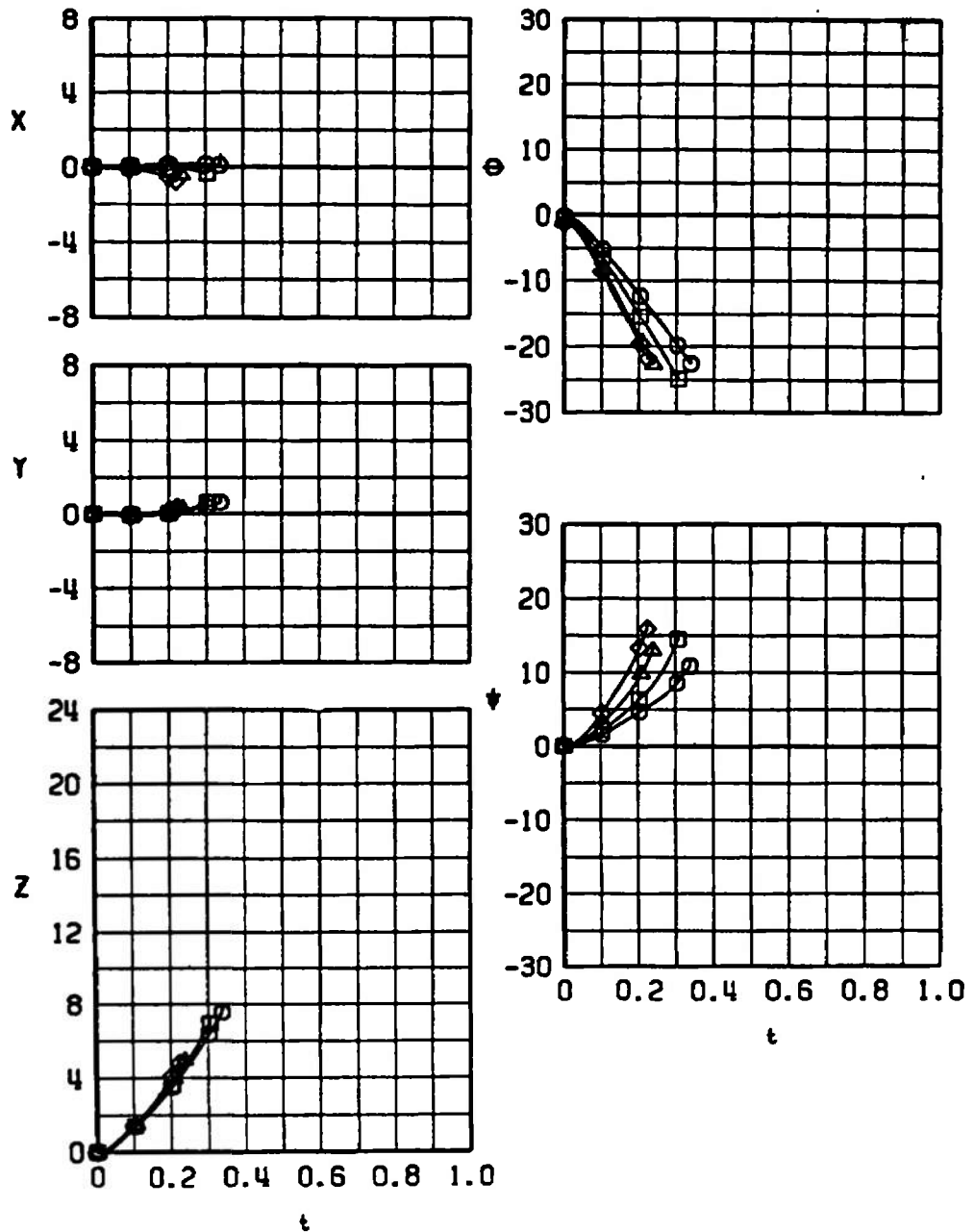
b. θ̄ = -45 deg
Fig. 22 Concluded

SYM	CONF	M_∞	α	H	$\bar{\theta}$
⊡	6	0.74	1.0	5000	0
△	6	0.82	0.5	5000	0
◇	6	0.90	0.2	5000	0
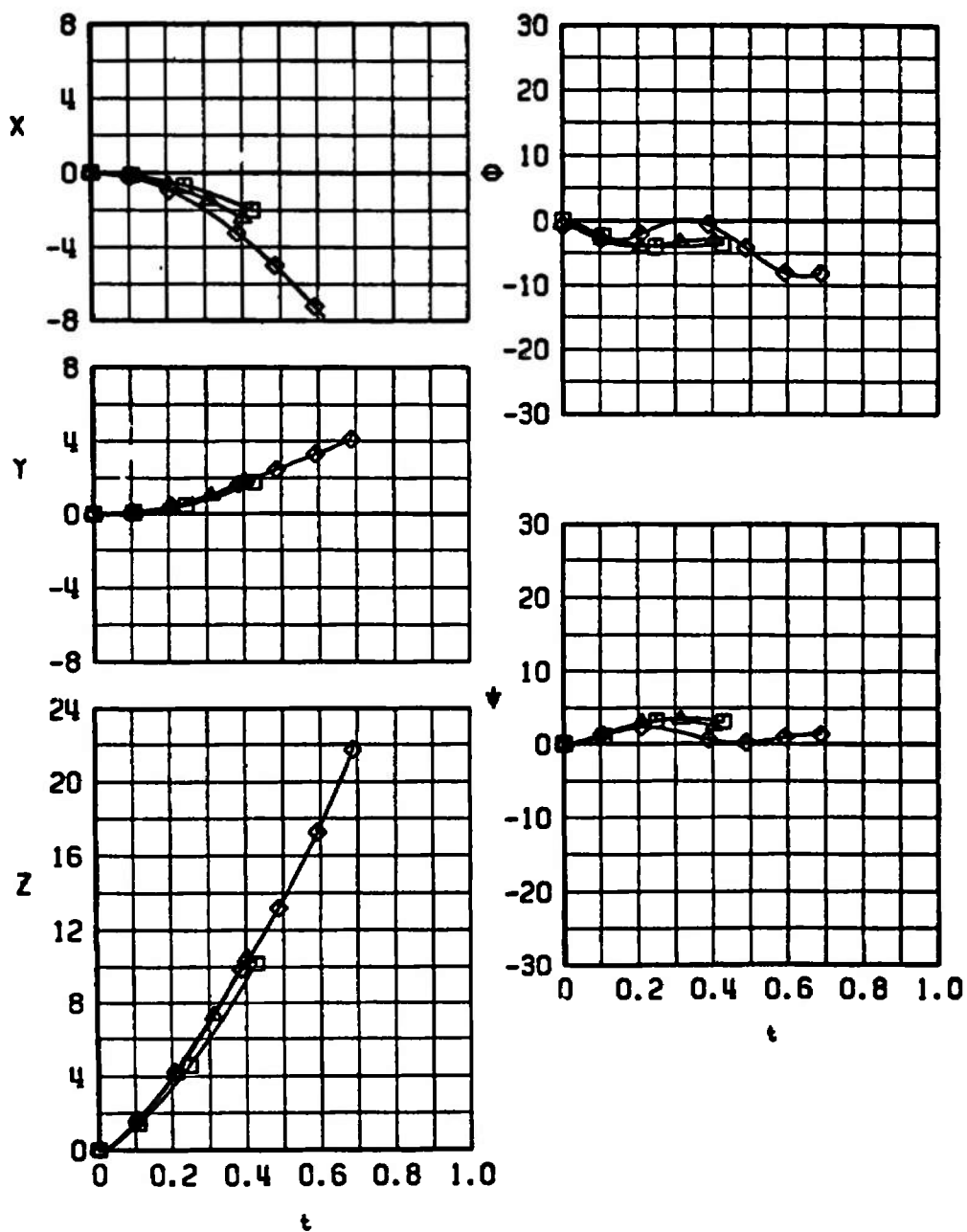
a. $\bar{\theta}$ = 0 deg

Fig. 23 Separation Trajectories from Right-Wing Inboard Pylon;
Fins Deployed

46

SYM	CONF	M_∞	α	H	$\bar{\theta}$
□	6	0.74	0.4	5000	-45
△	6	0.82	0.0	5000	-45
◇	6	0.90	-0.2	5000	-45
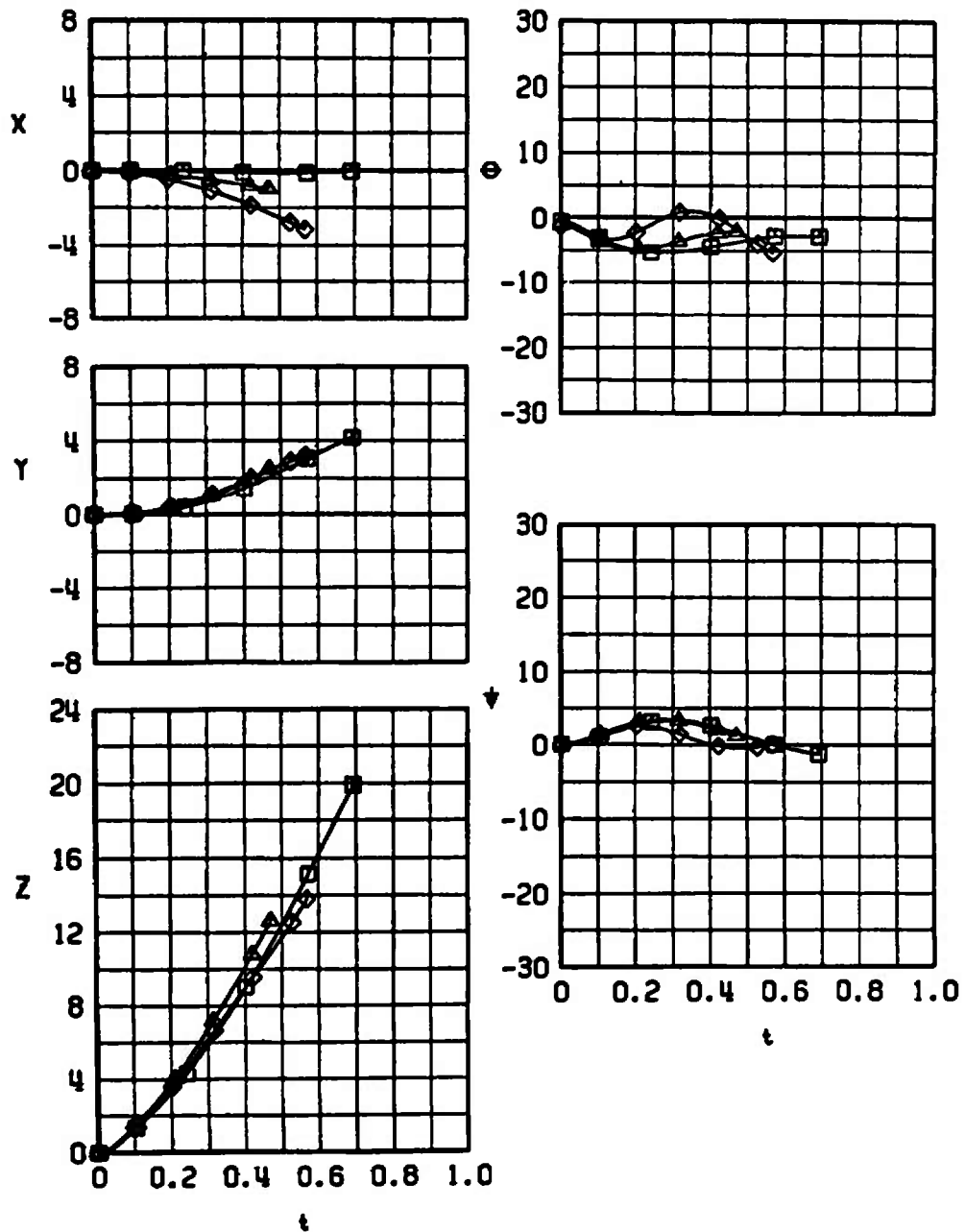
b. $\bar{\theta}$ = -45 deg

Fig. 23 Concluded
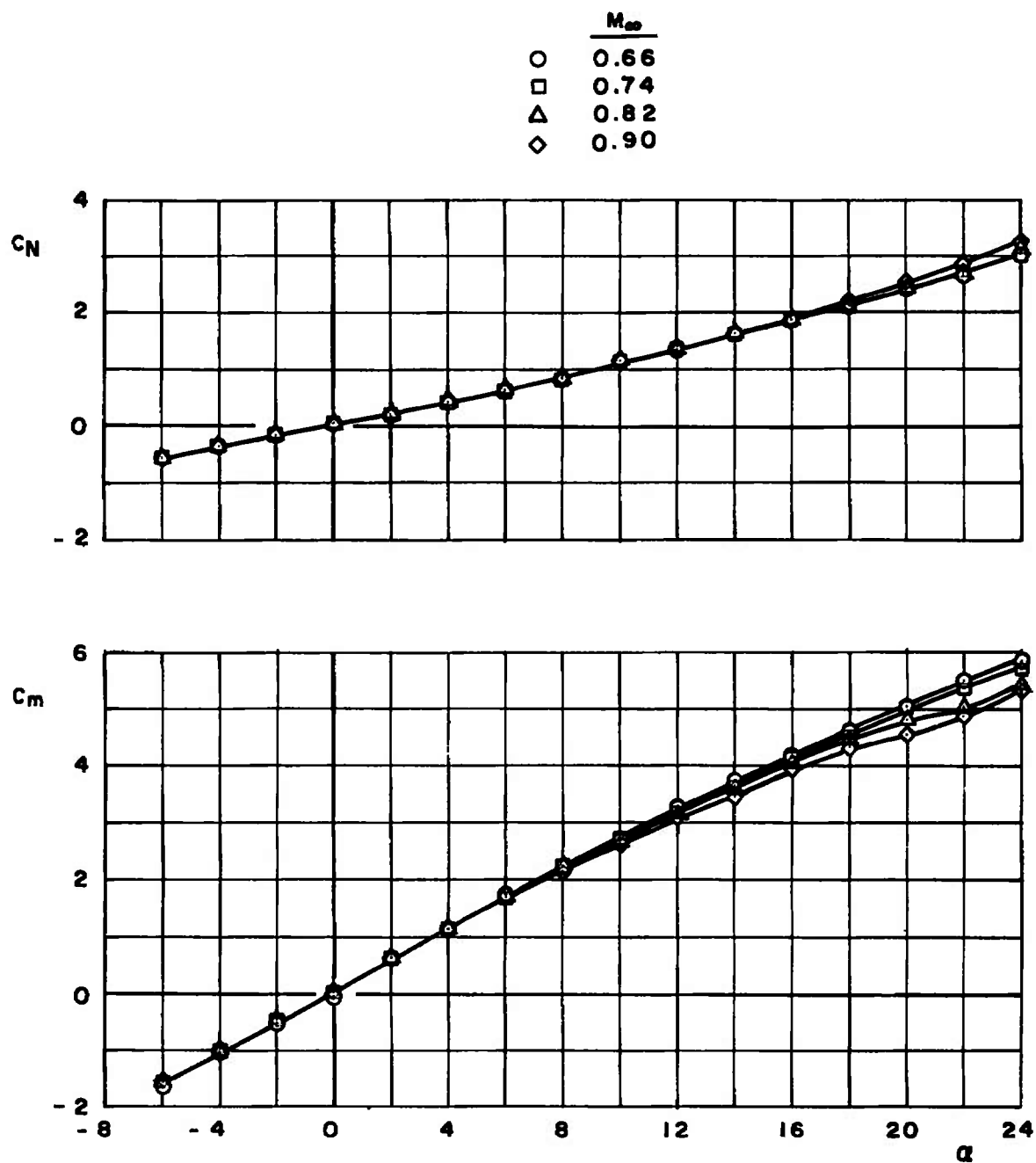
a. Fins Folded
Fig. 24 Free-Stream Static Stability Data for the GRM

b. Fins Deployed
Fig. 24 Concluded

TABLE I
FULL-SCALE STORE PARAMETERS USED IN THE TRAJECTORY CALCULATIONS

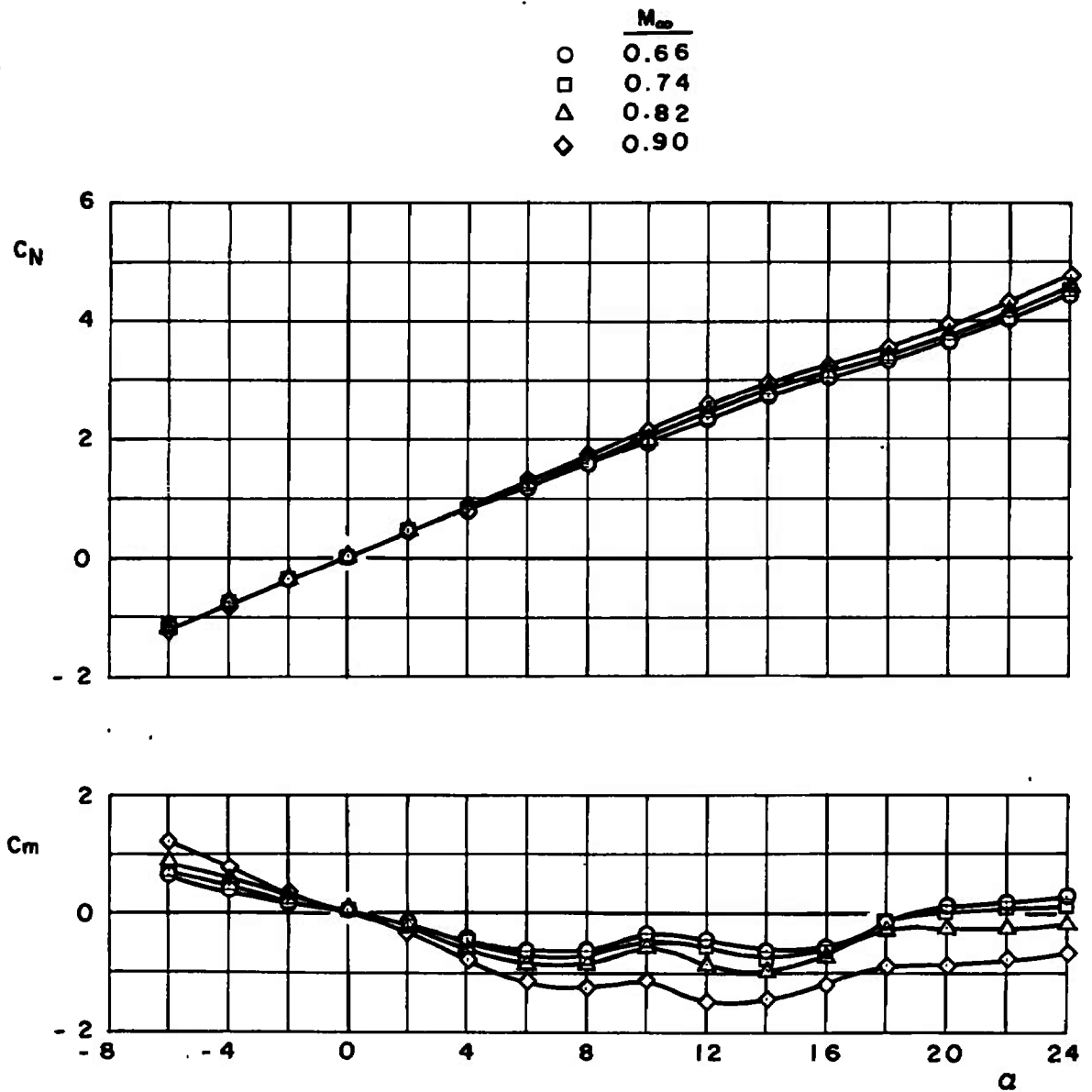| Parameter	Multiple Carriage		Single Carriage
	Folded-Fin Configuration	Open-Fin Configuration	Open-Fin Configuration
Mass, $\overline{m}$, slugs	18.090	18.090	18.090
Center-of-gravity location, X_{cg}, ft	7.033	7.033	7.033
Center-of-gravity location above the store axial centerline, ft	0.0108	0.0108	0.0108
Location of ejector force, ft			
X_L	0.041	—	—
X_{L1}	—	—	1.046
X_{L2}	—	—	0.621
Ejector stroke length, Z_E, ft	0.2552	—	—
Store reference area, S, sq ft	0.9503	0.9503	0.9503
Store reference diameter, b, ft	1.100	1.100	1.100
Pitch moment of inertia, I_{yy}, slugs-sq ft	113.841	113.841	113.841
Yaw moment of inertia, I_{zz}, slugs-sq ft	113.841	113.841	113.841
Product of inertia, I_{xz}, slugs-sq ft	0	0	0
Pitch-damping derivative, C_{m_q}, per radian	-160	-320	-320
Yaw-damping derivative, C_{n_r}, per radian	-160	-320	-320

TABLE II
MAXIMUM FULL-SCALE POSITION UNCERTAINTIES
RESULTING FROM BALANCE PRECISION LIMITATIONS

M_∞	t, sec	ΔX, ft	ΔY, ft	ΔZ, ft	$\Delta\theta$, deg	$\Delta\psi$, deg
0.66	0.2	±0.02	±0.01	±0.01	±0.1	±0.2
	0.4	±0.06	±0.05	±0.03	±0.5	±0.9
	0.6	±0.14	±0.12	±0.07	±1.2	±2.0
0.74	0.2	±0.02	±0.02	±0.01	±0.2	±0.3
	0.4	±0.08	±0.07	±0.04	±0.7	±1.1
	0.6	±0.18	±0.15	±0.09	±1.5	±2.5
0.82	0.2	±0.02	±0.02	±0.01	±0.2	±0.3
	0.4	±0.10	±0.08	±0.05	±0.8	±1.3
	0.6	±0.22	±0.19	±0.11	±1.8	±3.0
0.90	0.2	±0.03	±0.03	±0.01	±0.2	±0.4
	0.4	±0.12	±0.10	±0.06	±1.0	±1.6
	0.6	±0.26	±0.22	±0.13	±2.2	±3.6

DOCUMENT CONTROL DATA - R & D

(Security classification of title, body of abstract and indexing annotation must be entered when the overall report is classified)

1 ORIGINATING ACTIVITY *(Corporate author)*	2a. REPORT SECURITY CLASSIFICATION
Arnold Engineering Development Center ARO, Inc., Operating Contractor Arnold Air Force Station, Tennessee	UNCLASSIFIED
	2b. GROUP N/A

3 REPORT TITLE

SEPARATION CHARACTERISTICS OF THE MK-20 (ROCKEYE) LASER-GUIDED DISPENSER MUNITION FROM THE F-4C AIRCRAFT AT MACH NUMBERS FROM 0.66 TO 0.90

4 DESCRIPTIVE NOTES *(Type of report and inclusive dates)*

Final Report - May 10 to 13, 1971

5 AUTHOR(S) *(First name, middle initial, last name)*

J. R. Myers, ARO, Inc.

6 REPORT DATE	7a. TOTAL NO. OF PAGES	7b. NO OF REFS
August 1971	59	1

8a. CONTRACT OR GRANT NO F40600-72-C-0003	9a. ORIGINATOR'S REPORT NUMBER(S)
b. PROJECT NO. 1120	AEDC-TR-71-167 AFATL-TR-71-96
c. Program Element 64724F	9b. OTHER REPORT NO(S) *(Any other numbers that may be assigned this report)*
d. Task 09	ARO-PWT-TR-71-116

10 DISTRIBUTION STATEMENT Distribution limited to U.S. Government agencies only; this report contains information on test and evaluation of military hardware; August 1971; other requests for this document must be referred to Armament Development and Test Center (DLGC), Eglin AFB, Florida 32542.

11. SUPPLEMENTARY NOTES	12. SPONSORING MILITARY ACTIVITY
Available in DDC	ADTC (DLGC) Eglin AFB, Florida 32542

13 ABSTRACT   Wind-tunnel tests were conducted using 0.05-scale models to investigate the separation characteristics of the MK-20 Laser-Guided Rockeye Munition (GRM) from the F-4C aircraft. The separation trajectories were initiated from the right-wing inboard pylon utilizing the Triple Ejection Rack and from single carriage positions on the right-wing inboard and outboard pylons. Captive-trajectory store separation data were obtained at Mach numbers from 0.66 to 0.90 for parent-aircraft level flight and 45-deg dive angle at a simulated altitude of 5000 ft. Free-stream force and moment data were also obtained for the GRM with fins folded and deployed at Mach numbers from 0.66 to 0.90 at store angles of attack from -6 to 24 deg. For the time period of the trajectories obtained, the store separated from the parent aircraft without store-to-parent contact. Trajectory termination was usually a result of limitations imposed by the travel limits of the store support system or a balance load limit.

Distribution limited to U.S. Government agencies only; this report contains information on test and evaluation of military hardware; August 1971; other requests for this document must be referred to Armament Development and Test Center (DLGC), Eglin AFB, Florida 32542.

This document has been approved for public release its distribution is unlimited. *TAB 74-16, 2 august 74.*

DD FORM 1473 1 NOV 65

14. KEY WORDS	LINK A		LINK B		LINK C	
	ROLE	WT	ROLE	WT	ROLE	WT
separation						
trajectories						
scale models						
MK-20 (Rockeye)						
F-4C aircraft						
Mach numbers						
altitude simulation						

Arnold AFS Tenn